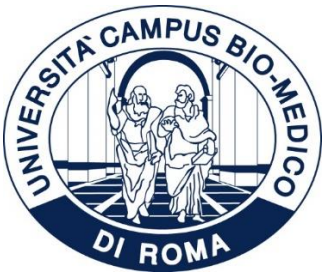

Campus Bio-Medico University of Rome

Ph. D. in Science and Engineering for Human and the Environment

XXXIII cycle a.y. 2017-2018

Invasive and non-invasive methods to elicit sensory feedback: a computational approach

Mattia STEFANO

Coordinator:

Prof. Giulio Iannello

Supervisor:

Prof. Loredana Zollo

Co-Supervisor

Dr. Eng. Francesca Cordella

ABSTRACT

Upper limb neuroprostheses are innovative interfaces that combine two properties, the possibility to be controlled by the subject and the possibility to deliver sensations to the subject related to the external environment or to the interaction with objects. Actually these devices can be controlled by processing electromyographic signal extracted from muscular activity of the arm. To deliver sensations, different techniques can be used. One of the most explored and promising techniques is the neural electrical stimulation: electrical stimuli are directly delivered to the residual nerves of the forearm to restore tactile sensation similar to the natural ones. Because of the high invasiveness of this technique, it can be useful to study it by means of computational models to evaluate the interaction between the nerve and electrode, to estimate optimal stimulation parameters and to design novel interfaces.

Another technique to restore sensory feedback, is the Focused Ultrasound Stimulation applied to the Central Nervous System. Also the study of this technique in simulation environment is important because of its possibility to damage tissues related to the high power intensity delivered.

The aim of this Ph.D. thesis is to study and discuss these techniques in simulation environment. A review study on the main modeling and computational frameworks adopted to investigate peripheral nerve stimulation is performed. Mathematical models of neural cells with a detailed description of ion channels and numerical simulations using finite element methods (FEM) to describe the dynamics of electrical stimulation by implanted electrodes in peripheral nerves are treated. Different cell models with different ion channels present in neurons are evaluated to provide a guideline on multiscale numerical simulations of electrical nerve fibers stimulation.

The interaction between electrode stimulation and nerve fibers is studied to evaluate the ability to activate fibers. DS-FILE intraneural electrode is considered in the FEM simulation to study its interaction with nerve fibers. The results can be very useful for the advancement of more realistic tactile sensations in amputee subjects from two point of view: the efficacy of the stimulation, that is related to the activation of axons subjected to the electrical stimulation, and the safety of the stimulation, related from a first consideration to the current intensity and waveform used. Therefore, the results of three type of waveform, that are the more safe as reported in literature [1], are analyzed and compared. The research aims to study, by means of a FEM-Neuron computational model, the axon fibers activation by means of the in-

traneural stimulation using different types of stimulus waveforms. The obtained results show that, using a biphasic charge unbalanced stimulus, the threshold to activate all the fibers considered in a location near an active site of the electrode is lower than the threshold found using biphasic charge balanced stimuli. This is an important result because the stimulation is equally efficient using low current amplitude.

The three different types of stimulation waveforms (i.e. biphasic charge balanced stimulus with inter-pulse delay, biphasic charge balanced stimulus without inter-pulse delay, biphasic charge unbalanced stimulus with inter-pulse delay) are also considered in three different nerve fascicles, i.e. two sensory and one motor fascicle at ten distances from the electrode in the fascicles.

The efficacy of the stimulation, expressed as the percentage of activation of the fibers, and the safety, in terms of current intensity and used waveform, are studied in the previously described different conditions and the results are compared. The obtained results show that: i. stimulating a sensory fascicle with implanted active sites can activate a fascicle close to it, but not all the fascicles belonging to the same nerve. In fact, in the nerve considered in the study, a motor fascicle cannot be activated due to the values of the electrical potential which are too low to activate the fibers; ii. the current intensity necessary to activate fibers increases according to the distance from the source of the stimulus; iii. by using a biphasic charge unbalanced stimulus, the threshold to activate the fibers is lower than using the other tested waveforms. It is an important result because the stimulation is efficient but safer since current intensity is lower than the one used for the other two waveforms.

Another important aspect to be evaluated is the computational time to find the solution of the FEM-Neuron simulations. Often, a high computational simulation time is also related to the complexity of the model geometry; therefore using a geometrical simplified model can be an important aspect to be analyzed. The aim is to deepen, the possibility of approximating a realistic 3D human median nerve model, based on anatomical imaging to a simplified model using hybrid FEM-Neuron approach. So the simplified model is built approximating inner fascicles shape to simple geometrical shapes, i.e. ellipses.

The results obtained allow concluding that the percentage of activation ranges at different distances from the active site obtained by the two model are comparable.

The hybrid FEM-Neuron computational models can be also used to study fibers activation in human median nerve with the aims of evaluating differences in activation obtained by using ds-FILE and cuff electrodes and comparing simulation results with experimental evidence in a human amputee.

The obtained results show that: i) fiber activation into the fascicles increases with the electrical charge, starting from the fascicles closer to the active site; ii) current amplitude necessary to activate fibers using the cuff electrode is higher than for the ds-FILE; iii) comparing the results of simulation with the experimental ones, it can be assumed that the increase of the intensity sensation in the amputee subject corresponds, in the simulation framework, to an increase of number of fibers activated in one or more fascicles. The simulation study on transcranial Focused Ultrasound Stimulation (tFUS) technique aims at evaluating, by the means of a computational model, the maximum pressure and the average acoustic intensity generated by a pulsed tFUS stimulation waveform, whose duty cycle (DC) is modulated in the range from 100% to 40%. The main goal is to investigate the efficacy and the safety, respectively in terms of pressure and intensity, of the stimulus waveform when the DC is decreased. Moreover, the Full Width at Half Maximum (FWHM) intensity at the focus is observed.

The obtained results showed that the amount of average acoustic intensity decreased with the DC and the maximum pressure remains constant. Therefore, low value of DC permits to effectively and safely extend the stimulation duration. Moreover, the FWHM did not vary during DC modulation; hence, the spatial resolution of the focus remained unchanged. These results suggest that tFUS can be adopted to safely stimulate the somatosensory cortex, properly modulating the stimulus duration, in order to elicit different sensations in the human hand.

CONTENTS

LIST OF FIGURES

LIST OF TABLES

1 INTRODUCTION

Neuroprostheses are a promising and widely investigated solution for human nervous system injuries, disorders and disabilities. Thanks to these devices, an improvement of the quality of life of the patients can be reached. Neuroprosthetic devices are used for different kind of disease. For example, parkinson [2], migraine [3] and other central nervous system diseases can be treated by Deep Brain Stimulation. Furthermore, neuroprosthesis also include retinal implants, to overcome some forms of blindness [4], or in case of spinal cord injuries to provide spinal cord stimulation for motor rehabilitation [5].

Thanks to neuroprosthetics, also upper limb amputees can obtain improvements in their quality of life. Nowadays, the most used upper limb prosthesis are myolectric devices. They allow to decode muscle electrical activity, recorded by myoelectric electrodes, and to provide patient with only an efferent control. These devices do not provide afferent information [6, 7], which are instead fundamental to interact with the environment.

As reported in literature [6], the lack of sensory feedback is one of the main reasons for the prosthesis use abandonment. The possibility to have a sensory feedback is a quality widely required by amputees to improve the dexterity and the embodiment of the robotic prosthetic hand [7]. Thanks to this solution, amputee subjects could obtain information from the environment and interacting objects. They could have information from the manipulation of objects about its shapes and dimensions, or distinguish different surface pattern textures [8, 9].

Therefore, several solutions for delivering sensations related to tactile feedback were proposed in the field of upper limb neuroprosthetics, such as electrotactile, vibrotactile, direct current stimulation, etc.. Among them, the electrical neural stimulation of peripheral nerve is the technique that more than the others allows to restore sensory feedback eliciting sensations similar to the natural ones [10–12]. In order to electrically stimulate the nerves to restore sensory feedback, different interfaces were developed, such as intraneural or extraneural electrode like cuff or flat model interfaces. These solutions based on electric current stimulation are applied to residual peripheral nerves (median and ulnar nerve) of the amputee foreharm.

Other techniques, different from the direct current stimulation of peripheral nerves are also used to restore sensory feedback in patients. Some of these can be applied to peripheral or central nervous system. Recently, one of the most used techniques is the focused ul-

trasound stimulation. Many studies are related to the stimulation of central nervous system, in particular to primary and secondary somatosensory cortex (S1,S2), using the transcranial focused ultrasound stimulation (tFUS). Using this technique, works demonstrated the possibility to elicit different sensations related to pain or tactile sensations on the hand and foreharm of the human subjects. [13, 14]. The FUS technique can be also applied to upper limb peripheral nerves with the same aims, i.e. elicit tactile sensations. The differences between tFUS and peripheral FUS are related to stimulation transducers used that involves different stimulation parameters.

The electric current neural stimulation permit to elicit tactile sensation more similar to the natural one, but because of the high invasiveness could be useful to study the nerve-electrode interaction from a computational point of view, by using simulations. Many research studies in the last years used this type of approach [3, 15–18]. Thanks to the simulations results, optimal parameters and location of the electrode in the nerve could be derived, to obtain better fibers recruitment related to the tactile sensation to be provided to the amputees. Studying stimulation parameters and electrode implant properties in computational simulations can provide a guide line to the experimental tests and to design new generation of electrodes and novel interfaces suitable for sensory feedback restoring.

In a similar way, although the FUS techniques is a non-invasive method, attention needs to be paid to the power intensity applied on the target area. For instance, the temperature increases due to the acoustic intensity could damage tissues if not kept below a safety threshold. Therefore, the signal intensity and the stimulation duration cannot overcome safety limits. So it is evident that a preliminary study of FUS outcome in simulation environment is extremely important.

The aim of this Ph.D. thesis is to study, in simulation environment, two of the main techniques used in literature to restore sensory feedback: electric current stimulation of peripheral nerves by means of neural electrodes; tFUS on Central Nervous System.

To study nerve-electrode interaction 3D human median nerve and two different type of neural electrodes (ds-FILE and cuff electrode) are developed. Multiscale approach is considered using Finite Element Methods (FEM) to study the distribution of electric potential into the nerve and Neuron environment to couple the FEM results with mathematical models of axons. Ultrasound stimulation is studied in a 2D simplified human head model in order to investigate the maximum pressure amplitude, the mean intensity and the focus profile for different Duty Cycle (DC). Simulations are performed using k-space pseudospectral method-based solver, i.e. k-Wave [19]. The contribution of this thesis is to study the electrical current stimulation

and FUS methods to restore sensory feedback in upper limb amputee subjects using mathematical models and computer simulations.

In this Ph.D. thesis, computational simulation approach is used to study: i) nerve-electrode interaction related to the neural current stimulation; ii) effect of tFUS through skull and brain tissue models. The work is structured as follows:

- In Chapter 2 the state of art of the most commonly used mathematical models of axons is treated, with a specific focus on developing multiscale computational model to study nerve-electrode interaction. So ion channels found in animal and human axon fibers, and the mathematical models of axons found in literature are discussed. Subsequently, approaches in building a multiscale model by coupling the microscale mathematical models of axons and nerve dynamics to the macroscale modeling of fascicles stimulation are considered. Part of contents of this chapter are published in [20].

- In Chapter 3 multiscale simulations are used to study nerve-electrode interaction in 3D human median nerve model. Different stimulation waveform are analysed to study their safety and efficacy. Fibers activation is studied at different distances from the active site in two different sensory fascicles and in a motor fascicle to know the possible spatial range of fibers activation using a particular model of intraneural electrode (ds-FILE electrode). Subsequently a 3D simplified human median nerve model is considered, approximating the inner fascicles to elliptical section shape. A comparison in terms of fibers activation, between the anatomical and simplified median nerve model subjected to the current stimulus is studied. Part of contents of this chapter are published in [21–23].

- In Chapter 4 the multiscale approach is used to study fibers activation using ds-FILE and cuff electrode in 3D model of human median nerve. Fibers random population into the nerve fibers is considered and a comparison between simulation results and experimental studies on human amputee are performed.

- In Chapter 5 a computational analysis to predict tFUS propagation in biological tissue is considered to study safety and efficacy of the stimulation. Maximum pressure and power intensity results obtained from the k-Wave acoustic simulation tool are discussed considering propagation in free water and in brain tissue through the skull layer at different values of duty cycle. Part of the contents of this chapter are published in [24].

- In Chapter 6 conclusions and final considerations are reported.

2

THE MULTISCALE APPROACH TO AXON AND NERVE STIMULATION USING MATHEMATICAL MODELS AND SIMULATIONS

2.1 INTRODUCTION

As discussed in Chapter 1, electrical nerve fiber stimulation is a technique widely used in prosthetics of upper [25] and lower [26] limbs and in therapeutic applications for neural disease treatment [16]. Recently, in the framework of upper limb prosthetics, invasive techniques to electrically stimulate peripheral nerves were used to elicit tactile feedback [7].

Computational models represent a useful tool to study electrical nerve fiber stimulation properties. In particular, advanced mathematical modeling is needed to achieve greater insights on the biophysical mechanisms driving nerve stimulation, overcoming experimental limitations, like high invasiveness and the in-vivo experiment on animals. Comprehensive models are also necessary for predictions on implant success and can be easily fine-tuned in a personalized medicine framework.

In the literature, some papers deal with electrical nerve fiber stimulation using a computational approach [15–18, 27], aiming to forecast the tissues response to the implanted electrode and to evaluate the current stimuli properties considering the tissue characteristics.

To this purpose, detailed microscale neural cell electrical models are combined with macroscale FEM in a multiscale framework. The modularity of the multiscale description guarantees flexibility concerning the particular stimulating device, the coupling between the macroscale and microscale descriptions, the geometry and type of fibers, up to the ion channels and electrical dynamics of nerves. The resulting computational framework can be used to design and test different types of electrodes, varying geometry, materials, and position of active sites, investigating the electrical dynamics of neural cells when an electrical current is applied.

PROGRESS BEYOND THE SOA The contribution of this chapter is to provide a review study on the principal mathematical axon models used in literature. To the best of our knowledge, there are not review studies in the literature on axon and nerve stimulation modeling based on such multiscale approaches. Therefore, it is expected that this chapter can give valuable information to the researchers aiming to develop comprehensive simulations on electrical stimulation of

peripheral fibers, with important applications in prosthetic.
With these premises, Chapter 2 aims to in-depth analyse and compare the most used computational models of nerve fibers, paying attention to the animal experimental data used to validate the theoretical model, the myelin sheath presence, and the different type of ion channels considered for each discussed model. Moreover, this chapter wants to provide a guideline to develop a multiscale model, which integrates the microscale description of nerves dynamics with macroscale numerical simulations and considers electrodes and volume-conduction in tissues.

Chapter 2 is structured as follows: First of all in Section 2.2, an overview of the biophysics and ion channel properties of axons, as the different animal models vary, is presented. Secondly in Section 2.3, mathematical models of axons considering different arrangements of ion channels according to the corresponding animal model are discussed, giving the reader a perspective on the axons mathematical models used until now. The last section (Section 2.4) deals with the coupling between neural cell models and FEM-based modeling of fibers stimulation to obtain a multiscale computational framework of the studied case.

Papers were selected from literature with special attention to studies related to computational models of electrical nerve fibers stimulation with application in prosthetics framework, computational models that consider the coupling between mathematical neural cell models and finite element methods simulations, mathematical models of electrical stimulation of neural cell with experimental validation in animals or humans.

Literature research updated to July 2020 was performed using the Google Scholar and PubMed databases. The following keywords were used for the research: *Computational nerve stimulation model*, *Computational axon model*, *ion channels in axons*. All the considered publications were in English language. To select publications relevant to this review aims, the following inclusion criteria were considered: studies related to prosthetics, studies that use electrical nerve fiber stimulation on peripheral nerves, studies on mathematical models of axons. Papers addressing the inclusion criteria were selected. From the initial 160 papers, 85 have been excluded since they did not meet the inclusion criteria. 75 full papers were assessed for eligibility, and 40 papers were excluded since not related to peripheral fibers. A systematic analysis of the remaining 35 papers have been performed (Figure 1).

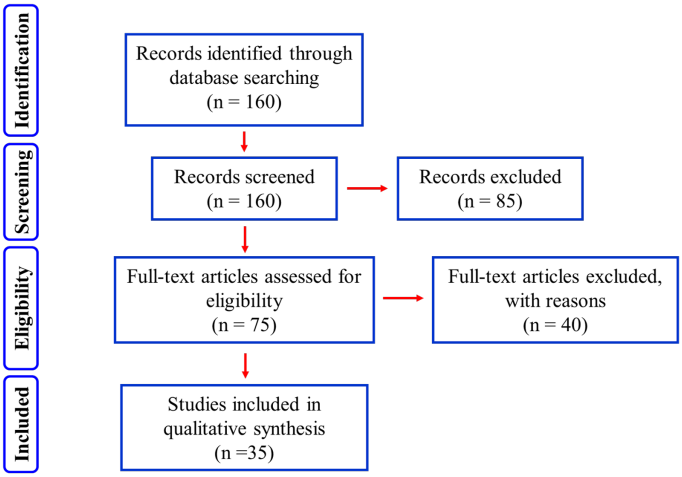

Figure 1: Flow-diagram of the papers search [28]

2.2 ION CHANNELS IN UNMYELINATED AND MYELINATED AXONS

In this section, ion channels in unmyelinated and myelinated axons are treated in detail. Ion channel expression and distribution in the most investigated animals are considered. Animal species such as mouse, rat, and rabbit are further studied both to account for *in silico* modeling in animals and because of similarities, about neural cells, with humans, i.e., homologous ion channels. Moreover, a large amount of experimental data on animals can be found in the literature to be used for model fine-tuning, parameter optimization, and validation. In the literature, several works studying nerve fibers and neural cells from an experimental point of view, also considering ion channels concentrations changes with respect to spatial location on neurons, are proposed. In particular, a detailed description of anatomical and physiological properties of a generic neural cell, so as of ion channel in mouse, rat, and rabbit nerve fibers is provided. This information will be useful to develop mathematical models of neural cells of the related mammalians.

2.2.1 *Ion channel in mammalian nerve fibers*

ION CHANNELS IN MOUSE FIBERS It is known that there are some resemblances between ion channels in mouse and human. $Na_v1.1$, $Na_v1.2$, $Na_v1.3$ and $Na_v1.7$ channels are encoded by genes that can be found on chromosome 2 in mice and humans, while $Na_v1.5$, $Na_v1.8$ and $Na_v1.9$ are encoded by other type of genes. In PNS cells can be found $Na_v1.8$ and $Na_v1.9$, while $Na_v1.4$ and $Na_v1.6$ can be found in skeletal muscle and in CNS respectively [29]. In the PNS, axons are put in fiber fascicles to form peripheral nerves. The function of peripheral axons is to propagate action potentials to regions far from

the body of the cell. Generation and propagation of the action potential happen thanks to voltage-gated (VG) Na^+ and K^+ channels.

In peripheral axons, there are also VG Ca^{2+} channels. *In vitro* studies on mouse sciatic nerves show that if axons are electrically stimulated by pulses, a transient increase in intra-axonal Ca^{2+} concentration occurs along the axons due to the activation of N- and L- type VG calcium channels. So N-type and L-type VG Ca^{2+} channels mediate Ca^{2+} current in peripheral fibers. T-type VG ion channels are calcium channels activated by low voltage. They are present in the C-fibers, i.e. unmyelinated CNS and PNS nerve fibers PNS, and seem to be involved in modulation of action potential conduction velocity [30].

ION CHANNEL IN RAT NERVE FIBERS At juxtaparanodes in normal adult rat sciatic nerve, the K^+ channels $K_v1.1$ and $K_v1.2$ and the cytoplasmic $K_v\beta2$ are observed. Voltage-dependent K^+ channels are not observed in mammalian nodes of Ranvier, as discussed in the following paragraph about rabbit and in reference [31]. These channels can be found in paranodal and internodal regions. In rodents, peripheral nerves at Nodes of Ranvier $K_v7.2$ is observed. It can also be observed in motoneurons in the spinal ventral horn, while $K_v7.3$ is observed in myelinating Schwann cells. $K_v7.2$ and $K_v7.3$ are observed in nodes of small myelinated axons, $K_v7.2$, $K_v7.3$ and $K_v7.5$ are observed in unmyelinated somatic axons, in visceral unmyelinated axons, and in baroreceptor nerve terminals. K_v7 subunits, instead, are observed in peripheral nerves [32].

ION CHANNEL IN RABBIT NERVE FIBERS The first studies on mammalian using voltage-clamp techniques on nerve fibers were performed on rabbit [31] and rat [33]. From these studies, it was observed that the ionic currents in the rabbit node of Ranvier are a Na^+ current and a leakage current [31]. The Na^+ current is involved in the initial depolarization, and only the leakage current is involved in the repolarization since the K^+ current is not observed.

2.2.2 *Ion channels in humans*

In the following section, ion channel properties in human nerve fibers will be treated. From patch-clamp experimental studies on dissociated human axons, several types of VG sodium, VG potassium, and calcium-dependent potassium channels were found [34].
Previous research works pointed out different kinds of VG potassium channels in human peripheral myelinated axons [34, 35], among which: fast (F) channels which rapidly activate and deactivate, with a conductance $\gamma = 50\,\text{pS}$ [34]; slow (S) channels, characterized by slower kinetics, and conductance $\gamma = 10\,\text{pS}$ [35]; intermediate (I) chan-

nels, with a time constant intermediate between the values of the other two types of channel cited above, and a conductance $\gamma = 34\,pS$. In particular, K_v channel α subunits are grouped into 12 different subfamilies (K_v1-12), as observed in the mammalian genome. Among these 12 subfamilies K_v1, K_v3 and K_v7 can be found on axons. Along unmyelinated axons, at Axon Initial Segment (AIS), at juxtaparanodes of myelinated axons and in nerve terminals, $K_v1.1$, $K_v1.2$ and $K_v1\beta2$ can be found [36, 37]. VG calcium channels are involved in a large number of processes, such as the regulation of neurotransmitters release at nerve terminals, excitability, and firing patterns.

Concerning sodium channels, Na_v channels are involved in the initiation and propagation of action potential. Nine different α subunits, $Na_v1.1$-1.9, are encoded by mammalian genes, and, in addition, also auxiliary β subunits can be found. $Na_v1.2$ is observed in a small fraction of nodes of Ranvier in adult myelinated axons. $Na_v1.6$ can be found in both central and peripheral nervous systems. It is known that the Na_v channel α subunits found at the subcellular level is not the same for different types of neurons and different locations in the cell. In myelinated fibers, at the axon initial segment and at the terminal heminodes, $Na_v1.6$ can be found. $Na_v1.3$, $Na_v1.7$, $Na_v1.8$, $Na_v1.9$ can be found in peripheral sensory neural cells [38–41].

About calcium channels, T-type calcium channels open subjected to small perturbations from resting potential. In particular, $Ca_v3.2$ T-type channels can be found in central and peripheral neurons as well as in liver, cardiac tissue, and kidney. P/Q-type calcium channels also can be found in mammalian neural cells of PNS and CNS. $Ca_v2.1$ channels can be found at presynaptic terminals of the spinal cord, neuromuscular system, and brain. Calcium N-type channels can be found in CNS and PNS, in particular near synapses, here are involved in the process of the release of neurotransmitters. These ion channels are also involved in the amplification and integration of neural signals [42].

VG cation channels are responsible for generating the action potentials. The depolarization of the plasma membrane, i.e. a shift toward less negative values of membrane potential, triggers the action potential. In neurons, VG Na^+ channels opening is caused by a sufficient depolarization produced by a stimulus, so a small quantity of Na^+ enters into the cell following its electrochemical gradient. Other sodium ions are admitted, causing further depolarization, because of the influx of positive charge that depolarize the membrane. The process advances until the electric potential is increased from the resting value (around -70 mV) to a positive value of Na^+ equilibrium potential. At this point, other two mechanisms play important roles, the inactivation of Na^+ channels and the opening of VG K^+. Na^+ have an inactivating mechanism that induces the closing of channels even if the membrane is depolarized. Sodium channels remain in this in-

activated state some milliseconds until the membrane potential is returned to its resting value. So Na^+ can get three different states: closed, open, inactivated. This process happens in a local region of the plasma membrane, but the depolarization of the region can depolarize the neighboring regions which follow a similar process. The action potential can then propagate it as a traveling wave to involve all the plasma membrane. VG K^+ channels are responsible of a mechanism that bring the plasma membrane more rapidly toward its original potential value, so it can transmit another pulse. These channels open so the efflux of K^+ is verified driving the membrane toward the K^+ equilibrium potential, before that the inactivation of Na^+ channels is completed. The K^+ channels are affected by the membrane potential changes in the same way of Na^+ channels but with a slower kinetics [43] .

The location of principal ion channels is specified in Table 1 [36, 41]. Finally, it is worth noting that ion channels in human axons show analog features to homologous channels expressed in other mammals or even amphibians, and available data obtained on those species can be used to model axon dynamics in humans.

Table 1: Voltage-gated ion channels

Ion Channel type	Living organism	Location
Sodium channels		
$Na_v1.1$	Human	PNS
$Na_v1.6$	Human, Mouse	PNS
$Na_v1.7$	Mouse	PNS
	Human	Schwann cells
$Na_v1.8$	Mouse, Human	DRG
$Na_v1.9$	Mouse, Human	PNS
Potassium channels		
$K_v1.1$	Human	PNS
$K_v1.2$	Human	PNS
$K_v1.6$	Human	PNS
Calcium channels		
T-type	Human	PNS
P/Q-type	Human	PNS
N-type	Human	PNS

ION CHANNELS IN AIS The AIS (Figure 2) has particular electrical properties provided from VG ion channels collected densely [44]. In the AIS we can find:

i) Sodium channels: $Na_v1.1$, $Na_v1.2$ and $Na_v1.6$ isoform of sodium

channels can be found in the AIS. $Na_v1.1$ can be found in spinal cord motoneurons [45], in the AIS of retinal ganglion cells [46] and at the AIS of GABAergic neurons [47]. $Na_v1.6$ and $Na_v1.2$ are expressed in the AIS of myelinated and unmyelinated axons. $Na_v1.2$ is involved during development, then it is substituted by $Na_v1.6$ when myelination takes place [48, 49]. $Na_v1.2$ is conserved in the AIS of unmyelinated axons in adult neurons. Notably, Na^+ current density is greater in the AIS of the axon than in the soma [50]. Sodium currents are classified according to biophysical properties: fast inactivating Na^+ current I_{NaT}, the persistent Na^+ current I_{NaP}, and the resurgent Na^+ current [51].

ii) Potassium channels: Potassium channels $K_v1.1$ and $K_v1.2$ can be found in the AIS of inhibitory and excitatory, hippocampal and cortical neural cells, and are positioned more distally than $Na_v1.6$. $K_v2.2$ can be found at the initial segment of medial nucleus trapezoid neurons, while K_v7 channels are in the same region of axons of many central neurons.

iii) Calcium channels: Ca^{2+} channels regulate firing properties. T- and R-type VG Ca^{2+} channels can be found in the initial segment of Purkinje cells and neocortical pyramidal neurons and in the initial segment of brain stem cartwheel cells.

ION CHANNELS IN AXON TERMINAL The activation of chemical synapses is triggered by the opening of the $Ca_v2.2$ calcium channels and presynaptic $Ca_v2.1$. They can drive signal transmission in the axonal arborization. $Na_v1.2$, $K_v1.1$ and $K_v1.2$ can be observed at axon terminals. K_v3 can be found on excitatory and inhibitory neural cells, while K_v7 is observed on synaptic terminals and preterminal axons.

ION CHANNELS IN UNMYELINATED AXON $Na_v1.2$ sodium channels support the conduction of action potential. In unmyelinated fibers there are more than five voltage gated K^+ channel subunits [52, 53].

CHANNELS IN THE NODES OF RANVIER The signal conduction in myelinated axon is defined saltatory, and it happens thanks to node of Ranvier region, where sodium channels can be found. $Na_v1.1$ and $Na_v1.6$ are the subunits that are on nodes of Ranvier. In the node of Ranvier region, the density of $Na_v1.6$ is greater than the density found in the initial segment [54]. About the sodium currents found on the nodal region, there are persistent and transient macroscopic currents [55, 56]. Conduction along axons can occur thanks to $K_v1.1$, $K_v1.2$ channels in juxtaparanodal region, and $K_v3.1b$, $K_v7.2$ and $K_v7.3$ in the nodal region.

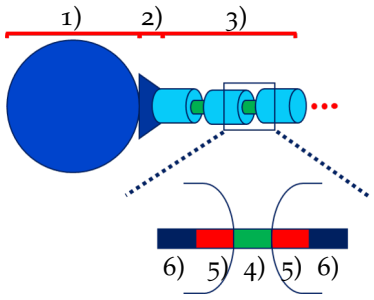

Figure 2: Scheme of myelinated neuron. 1) Soma; 2) AIS; 3) myelinated axon; 4) node; 5) paranode; 6) juxtaparanode.

2.3 MATHEMATICAL MODELS

In this section, the most used mathematical models of neural cells found in the literature will be analyzed. Such models describe the dynamics of membrane potential according to the ion channels observed in the corresponding cells from animals or human experimental data. Membrane voltage is studied to evaluate the activation of nerve fibers when subjected to an external stimulus. These models can be further included in a multiscale simulation by coupling to the stimulating device model, as will be described in the next section. In particular, based on the anatomical nerve fiber reconstruction and finite element methods, the electric potential distribution over the nerve fibers is evaluated given the stimulating electrodes parameters [22]. FEM model results can then be used as input to evaluate nerve fibers activation via the microscale axon biophysical model [21].

2.3.1 *Computational neuronal model*

Detailed biophysical neuronal models of axon dynamics represent a fundamental tool for investigating neurons response upon stimulation. They are based on axonal geometry modeling, ion current modeling, and internodal and nodal regions [57, 58]. Some theoretical models, starting from the work of McNeal [59], consider the myelin as a perfect insulator. In literature, the myelin sheath is treated according to three different considerations. The first one models the myelin sheath as a perfect insulator [59, 60], so the dynamics of the model is only defined by the membrane dynamics of the node of Ranvier. This configuration is equivalent to a single-cable electrical circuit model, where the axoplasm is modeled by a single resistor, Figure 3. Other models treat the myelin sheath as an imperfect insulator [57, 58, 61]. A series of compartments with resistors and capacitors in parallel can model the myelin sheath in a single-cable circuit model. Depending on the research aim, researchers use different types of axon models. The following paragraphs will analyze the most used mathematical

axon models: McNeal axon model, SENN model, Sweeney model, mSENN model, MRG model.

2.3.2 *Voltage-gated ion channels models*

VG ion channels can be modeled by two different methods: Hodgkin-Huxley (HH) or Markov schemes. HH scheme is the most used theoretical model to describe the electrical dynamics of neural cells, but we know that this theoretical model could be limiting in describing the dynamics of ion channels [62]. Markov model approach, in some specific cases, is a better description of the dynamics of ion channels.

According to the HH formalism, the membrane electric potential time change is described by the following equation

$$C_m \frac{dV_m}{dt} = -I_{ion} = -\sum_i I_i \tag{1}$$

where V_m is the membrane potential, C_m is the membrane capacitance, and I_{ion} represents the total transmembrane ion current, driven by different channel types i, also including the leakage channels. Stochastic processes dynamics can be studied by Markov models. They assume that the state of the system at a future time depends only on the current state, i.e., it is a memoryless process. Ion channels, according to the Markov model, are considered as a set of states [63]. Rate constants are defined to explain state transitions and can be related to membrane voltage or not. If we treat a gating variable as a two-state process, a HH model can be turned into a Markov model [64].

2.3.2.1 *Neural cell models*

Every research that proposed an HH model to describe ion channels gating is based on different voltage-clamp studies from amphibians, mammalians, or humans. The work of McIntyre et al. [65] used a model that has as a reference experimental voltage-clamp data from myelinated nerve fibers of rabbit sciatic nerve, from [66]. In that model, according to the experimental observations, there are not potassium channels. Kinetic parameters of the HH-type model are different according to the ion channels, and the physiology of the fibers studied. In the HH scheme, the ion channel current density related to each type of ion is considered. The ionic currents of the model can be written in the form

$$I_i = g_i(V_m - E_i) = \bar{g_i} \prod_j x_j^{p_j}(V_m - E_i) \tag{2}$$

where g_i is the maximum conductance for ion channels i ($\bar{g_i}$) multiplied by one or more gating variables (x_j), depending on activating and inactivating properties. E_i is the reversal potential, and p_j are

parameters used to match experimental data. The time evolution of each gating variable is given by

$$\frac{dx}{dt} = \alpha_x(1-x) - \beta_x x, \tag{3}$$

where, for voltage-dependent channels, α_x and β_x are functions of membrane potential and are estimated from experiments. α specifies the transition probability between the closed and the open states, while β is related to the transition between the open and closed states. Even if with different values of conductance and rate functions, most studies consider potassium and sodium currents, the most common currents found both in amphibian and in mammalian nerve cells. Also, by using HH models, it is possible to consider different ion current contributions, carried by specific channel types (sodium, potassium, or others), by opportunely fine-tuning electrophysiological parameters. In some instances, different types of potassium currents and conductances are considered to describe delayed rectifier K^+ current, slow non-inactivating K^+ current and different type of calcium currents: the high-threshold and low-threshold Ca^{2+} [67]. In several studies, only the difference between fast and slow potassium current is considered.

2.3.2.2 *Single ion channels*

Nowadays, several VG channels are known. In this section, we focus on the ion channels observed in axons: sodium and potassium channels α and β subunits, and N-type, T-type and L-type calcium channels. Some recent papers deal with the modeling of specific ion channels using the HH or Markov scheme. Balbi et al. [68] developed a kinetic model representing all α subunits of VG sodium channels. The kinetic model used is a Markov type model. Other studies consider some ion channels treated with the Markov scheme and other ion channels with the HH scheme. For instance, in the work of Feng et al. [69], for $Na_v1.6$ and $Na_v1.7$, a Markov type model is used, while an Hodgkin-Huxley type model is considered to model $Na_v1.8$ and $Na_v1.9$. Peters et al. [70] employed a HH scheme to describe the $Na_v1.1$ ion channel dynamics. They used the animal model of the Chinese Hamster and considered patch-clamp recordings at different temperatures from ion channels in ovary cells. $Na_v1.2$ and $Na_v1.6$ channels are described by using the HH scheme by Ye et al. [71]. In this study, patch-clamp recordings at different temperatures for sodium channels are considered.

The VG potassium channels are encoded by 40 genes. Some potassium channel kinetics and computational models are described by Ranjan et al. [72] and are found on Channelpedia [73]. In this framework, both Markov and HH computational models are considered.

VG calcium channels are grouped into three classes: T-type, N-type, and L-type. In the last years, L-type was the only known class: its

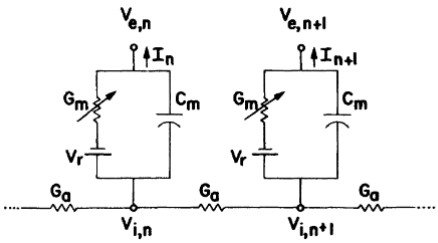

Figure 3: McNeal equivalent electric circuit scheme, from [59]. G_a is the axial internodal conductance, I_n is the membrane current at node n, $V_{e,n}$ is the external potential at node n, $V_{i,n}$ is the internal potential at node n, G_m is the nodal membrane conductance, C_m is the nodal capacitance, V_r is the resting potential.

ion current is also defined as long-lasting calcium current, and it needs a strong depolarization to be activated. N-type currents are only observed in nerves. T-type currents need weak depolarization to be activated and are observed in several cells. Notably, the activation mechanism is almost the same between Na^+ and Ca^{2+} channels [74]. The increase of intracellular concentration of Ca^{2+} ions or of membrane potential can lead to inactivation of L-type Ca^{2+} channels. Faber et al. [75] developed a Markov model of the L-type Ca^{2+} channel ($Ca_v1.2$) whose results are compared with experimental data from mammalians. Kinetics of L-type Ca^{2+} is also described by Alekseev et al. [76] using patch-clamp studies from ground squirrels.

In summary, all these ion channels models can be considered to build a neuron or axon model choosing the combination of ion channels depending on the physiological properties of the cell to be modeled.

2.3.3 *McNeal axon model*

The first model treated in this review is the simplest one: the McNeal axon model. McNeal [59] suggested a model of myelinated nerve fibers considering electrical properties of membranes after a stimulus application that induces the action potential. The McNeal model considers an equivalent circuit to simulate a myelinated nerve fiber (Figure 3). The approximations are the same as the FitzHugh studies [57], but McNeal considers the myelin sheath as a perfect insulator, fibers infinitely long, nodes of Ranvier regularly spaced, and geometrical properties consistent with the diameters of fibers. The electrical potential outside the fiber is related only to the stimulus current, the electrode geometry, and the tissue surrounding the nerve fiber. It is not affected by the fiber. In this study, a monopolar spherical electrode is considered, located 1 mm away from one node. The current stimuli are monophasic pulses. Fibers are considered of small dimen-

sions to simplify the model and assume that the membranes external surface at all nodes is equipotential. The outer medium with respect to the fibers is considered isotropic and infinite. The membrane voltage dynamics at the node n is described by the equation

$$C_m \frac{dV_n}{dt} + I_{i,n} = G_a(V_{i,n-1} - 2V_{i,n} + V_{i,n+1})\,. \tag{4}$$

The membrane conductance at nodes of Ranvier is constant when stimuli are subthreshold and before the action potential initiation. Only in the node of excitation the membrane dynamics follows the equation of Frankenhauser-Huxley for myelinated frog fibers [77]. The myelinated fiber can be described by the infinite set of linear first-order differential equations, substituting in Eq. (4) the ionic current at node n given by $G_m V_n$

$$\begin{aligned}\frac{dV_n}{dt} = \frac{1}{C_m}[G_a(V_{n-1} - 2V_n + \\ + V_{n+1} + V_{e,n-1} - 2V_{e,n} + V_{e,n+1}) - G_m V_n] \\ (n = 0, 1, 2, ..., N)\,,\end{aligned} \tag{5}$$

where $V_n = V_{i,n} - V_{e,n} - V_r$. $V_{i,n}$ and $V_{e,n}$ are the internal and external potential respectively at node n, G_a and G_m are the axial internodal and the nodal membrane conductances respectively, C_m is the membrane capacitance and V_r is the resting potential. The initial conditions are

$$V_n(0) = 0 \quad \forall n\,. \tag{6}$$

To obtain an approximate solution, it is possible to choose a finite set of differential equations related to the nodes involved and then integrate the set to compute the membrane potentials. The membrane model described in McNeal [59] considers only one node depolarized. At the stimulation node, defined as node 0, if we consider stimulus intensities close to the threshold or greater than it, the ionic current can be defined as

$$I_{i,0} = \pi d l (i_{Na} + i_K + i_P + i_L)\,, \tag{7}$$

where d is the axon diameter, l is the nodal gap width, i_{Na}, i_K, i_P, i_L are the ionic currents densities [77]. In this case, the term $G_m V_m$ in Eq. (5) is substituted by the term $I_{i,0}$.

2.3.4 *SENN computational axon model*

Reilly et al. [78] described another neuroelectric model based on the studies of McNeal. The model included nonlinear Frankenhauser-Huxley conductances at each node of Ranvier. This representation is the Spatially Extended Nonlinear Node (SENN) model. They studied

model results for two types of stimulus waveform: monophasic and biphasic waveform considering human and animal data. The SENN model is a middle ground between a simple single-node model, as the one treated in the previous paragraph, and a more complex node model with myelin representation. The response of the neuron to an extracellular stimulus can be studied by the equivalent electric circuit model. Electrical circuit components made of resistance, voltage source, and transmembrane capacitance, represent single nodes. The electrical characteristics of the myelin internode are not considered. Membrane conductivity is modeled as reported in the study of Frankenhauser-Huxley [77]. In this study, it is assumed that the current generated from the point electrode is isotropic, and the medium where the electrode is located is uniform. The axon considered has a diameter of 20 µm and internodal spacing of 2 mm. These geometrical properties, the medium, and fibers properties are assigned according to the work of McNeal [59]. The neuroelectric model permits the study of neural dynamics in response to different stimulus parameters, such as polarity, waveshape, and geometric properties related to the neural cell. In this way, the computational model can be used to forecast or guide experiments.

2.3.5 *Sweeney axon model*

Another compartmental cable model related to properties of mammalian myelinated fibers of peripheral nerves was developed by Sweeney et al. [60]. The model was built considering voltage-clamps studies on rabbit nodes of Ranvier. Also in this work, the nodes of Ranvier are represented by nodal capacitance and voltage-dependent ion channels Na^+ and leakage. As reported in the Section 2.2.1 about ion channels in rabbit nerve fibers, in the Sweeney et al. work, potassium ion channels are not considered. In their model, some similarities with the McNeal model are present: myelin sheath is considered as a perfect insulator. The cable is modeled with 19 compartments, a good choice to study conduction and excitation neglecting interference from the cable end (boundary conditions). Parameters are obtained from the literature, and temperature feedback is introduced via the Arrhenius factor. A rectangular current intracellular stimulus at the center node of Ranvier of a 10 µm diameter fiber model is considered to study properties of excitation. The electric potential time variation at a node is defined as

$$C_m \frac{dE_{m,n}}{dt} + I_{i,n} + \\ + \frac{1}{r_a}(E_{m,n-1} - 2E_{m,n} + E_{m,n+1}) + I_{inj,n} = 0\,, \quad (8)$$

where C_m is the nodal capacitance, $E_{m,n}$ is the membrane potential at node n, $I_{i,n}$ is the total ionic current at node n, r_a is the internodal

axoplasmic resistance, and $I_{inj,n}$ is the intracellular injected current at node n.

2.3.6 *mSENN axon model*

The two computational models analyzed above are used to describe the behavior of mammalian nerve fibers [79, 80]. Frijns et al. [81] developed a modified SENN model (mSENN) where the changes are in accordance with mammalian nerve fiber data found in literature, also considering the effect of temperature on nerve kinetics. Neurophysiological studies stated that the behavior of nerve fibers is related to temperature [82]: impulse conduction velocity, excitability, action potential amplitude, action potential duration in a nerve fiber are significantly affected by temperature. The temperature dependence can be included based on the Arrhenius equation and by multiplying the activation and inactivation rate constants by a factor ϕ defined as follows

$$\phi = Q_{10}^{(T-T_0)/10}, \tag{9}$$

where Q_{10} is a parameter fine-tuned to reproduce temperature-dependent variations as observed in experiments. In this study, besides the introduction of temperature dependence, geometrical properties of the nerve fiber were set to describe a motor fiber of 10 µm diameter. Therefore, taking into account the temperature effects and by introducing a realistic nerve morphology, they obtained a good fit between in vivo and simulated action potentials in terms of shape, duration, and conduction velocity. This model predicts the influence of physiological variations of body temperature on different features of the nerve behavior [81].

2.3.7 *McIntyre-Richardson-Grill (MRG) axon model*

In this case, there is a more complex representation of an axon, used to have more insight on mechanisms for depolarizing afterpotentials (DAPs) in myelinated axons [84, 85]. Paranodes, nodes, myelin, and internodes were modeled by using the corresponding electric circuit double cable model, where the myelin is considered as an arrangement of capacitances and resistors. Studies of Blight [86] and other double-cable models have been used in other works [87–90] for reproducing depolarizing afterpotentials.

Other works study how the myelin can affect the conduction and excitation properties of axons to select the better model to describe myelinated axons subjected to extracellular excitation [91]. Several computational models of nerve fibers were considered to describe the propagation of action potentials along the axons for myelinated or unmyelinated fibers. Computational axon models according to the

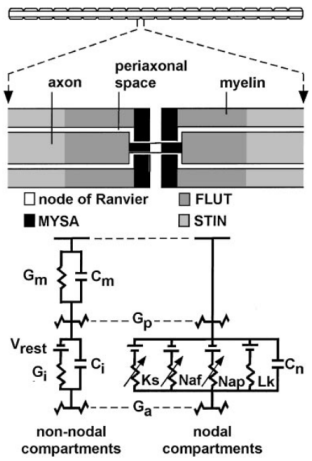

Figure 4: Double Cable axon model, equivalent electric circuit [83]. In this scheme are expressed myelin conductance and capacitance, G_m and C_m respectively, the rest potential V_{rest}, internodal conductance G_i and capacitance C_i, nodal capacitance C_n and conductances of the ion channels: slow potassium K_s, fast sodium Na_f, persistent sodium Na_p, linear leakage L_k. MYSA, myelin attachment segment; FLUT, paranode main segment; STIN, internode segment.

type of nerve cell, including soma, axon, and dendrites, or only axon, have been developed; they may differ depending on whether the cell belongs to the Central or Peripheral Nervous System.

More detailed models of mammalian motor nerve fibers have been developed to deepen the biophysical mechanisms involved in variations of axonal excitability and to control the recovery cycle. A work developed by McIntyre et al. [83] studies a double cable axon model, considering nodes of Ranvier, myelin sheath, paranodal and internodal sections Figure 4. Modeling results are nicely in agreement with experimental data on the excitation properties of mammalian myelinated nerve fibers. All the sets of ion channels at the node and the geometry of the paranode, internode, and myelin were needed to make more accurate the model description to the experimental data. The objectives of the study are related to the influence of afterpotentials on the recovery cycle, but it is interesting noting the properties of the double cable axon model. The geometry and membrane dynamics of the models were based on experimental measurements from human, cat and rat. In this study, 10 segments between two consecutive nodes of Ranvier are used, and myelin attachment segment (MYSA), paranode main segment (FLUT), and internode segment (STIN) regions of the fiber are introduced. By varying the fiber diameters from 5.7 to 16.0 µm, nine models were produced based on experimental measurements of the morphology.

The electrical response of the axons was reproduced by using models based on both linear and nonlinear formulations for membrane

voltage dynamics. To describe the dynamics of Nodes of Ranvier are considered nonlinear and persistent sodium conductances, potassium conductance, a leakage conductance, and the membrane capacitance. Previous experimental research studies [34, 35, 92] are considered to describe the dynamics of the ion channels in nodes of Ranvier. From other research studies, it was observed that slow K^+ channels are in the nodes of the mammalian myelinated axon [34, 35, 93]. The parameters about the kinetics of ion channels are considered to reproduce several experimental studies for different fiber diameters. The same dynamics of Richardson et al. [91] was used, with the modification of some parameters related to time constants and conductance density [83]. The accurate representation of fiber geometry and nodal membrane dynamics reproduced different experimental data.

2.4 SIMULATION ON STIMULATION TECHNIQUES

This section presents the current approaches in building a multiscale model by coupling the microscale mathematical description of axons and nerve dynamics to the macroscale modeling of fascicles stimulation. In particular, we discuss the different steps needed to obtain the multiscale model, considering the information presented in previous sections. After a mathematical neuron model has been built, to make a comprehensive model that describes the behavior of the nerve fiber subjected to an external stimulus, the anatomical properties and the interaction between tissues and stimuli have to be considered. The first step is to consider mammalian neural cells to model. In this way, it is possible to find the corresponding ion channels expressed in that cells, as treated in Section 2.2. Once the ion channels set to be included in the model is identified, it is possible to choose the preferred mathematical approach for ion currents dynamics and channel kinetics. Also, it has to be evaluated the axon model to adopt, based on the configuration of nodes, myelin sheath, and channel distributions. Notably, all axon models discussed previously can be generalized and personalized to include additional ion current components from different channels. For instance, the MRG axon model treated in Section 2.3 could be considered, but if it needs different ion channels, not considered in the MRG model, but observed from the experimental data about the mammalian, the new ion channels can be opportunely modeled and included in the current balance equation.
Concerning the macroscale modeling of the stimulation, several studies in the last years focused on FEM modeling to study the behavior of nerve fibers subjected to electrical stimuli from implanted electrodes [15, 16, 18, 94, 95]. In those investigations, numerical simulations are used to evaluate the electric potential distribution across the nerve fiber. Other studies use the same approach for different stimula-

tion techniques, such as Transcutaneous Electrical Nerve Stimulation (TENS) [94, 96].

The Finite Element model can be built starting from histological images of nerves [27, 97], from micro-computed tomography (μCT) anatomical studies [98] or magnetic resonance imaging (MRI) data of the subject so as to obtain more accurate results [18]. Following this approach, it is possible to have a more realistic model able to describe nerve-electrode interaction and to study properties of different types of electrodes [15, 99]. Therefore, for instance, it would be possible to investigate the interaction between electrodes and fibrotic tissues and evaluate the better solution for long term implants, and the placement of electrodes in the fibers to obtain more selectivity and fiber recruitment [15]. In the simulation environment, different types of electrodes and stimulation parameters can be tested, with the aim to design optimal stimulation strategies based on computed results, also considering the fibers behaviors. The first step of FEM modeling is the definition of the geometry. As aforementioned, the geometrical model can be built from the anatomical image or other types of data (MRI or computed tomography). Hence, using a FEM software, a 3D model of the anatomical components, including nerve fibers and other tissues, can be developed. In addition to the anatomical model, the electrode model has to be considered and developed. The CAD model of the electrode can be done starting from the technical properties of the specific electrode model, according to the aims of the application. For example, if we consider a peripheral nerve stimulation by intraneural electrodes, we can develop the CAD model according to the properties related to dimension and shape. After this step, the material properties can be assigned to different components: electrode and anatomical regions. Tissue properties can be assigned to different anatomical parts, included in the study. The specific material properties found in the literature are assigned at each region of the model to represent different tissue types. In general, considering peripheral nerve fiber, three different tissues are selected: epineurium, perineurium, and endoneurium. The intrafascicular endoneurium has an anisotropic conductivity tensor with a longitudinal value, and a transverse value [27, 97]. The epineurium and perineurium are assumed to be isotropic media. It is assumed that the nerve is surrounded by a homogeneous saline solution. Electrode models can be made using the same approach, modeling different materials and properties related to them. The physics related to the electrical stimulation problem is solved by integrating Maxwell's equations on the detailed domain presented above in a quasi-static approximation framework. This assumption can be made because of the intensity and duration of the stimuli related to nerve stimulation, as studied in [100]. From the finite element study, it is possible to obtain the electric potential and density current distribution in the nerve fiber after that an electric current is applied.

Recently, many works used this approach in the field of neuroprosthetics of upper and lower limb [15, 17, 27]. The electric potential or current data can be extracted from the simulation software and processed using a data analysis software. Subsequently, the electric potential can be used as the external (extracellular) potential for the neuron or axon models, selected among those cited in the previous sections. Based on the simulated fields, specific signals wave-forms can be built to introduce time-varying stimulations in the micro-scale model.

The equations to be solved in the FEM model are

$$\nabla \cdot \vec{J} = Q_j \tag{10}$$

$$\vec{J} = \sigma \vec{E} + \vec{J_e} \tag{11}$$

$$\vec{E} = -\nabla V \tag{12}$$

where $\vec{J}$, Q_j, $\vec{E}$, $\vec{J_e}$, and σ are the current density, the current source, the electric field, the external current density, and the conductivity tensor, respectively. Q_j and $\vec{J_e}$ are set to zero everywhere in the model. A Dirichlet boundary condition $V = 0$ is set at the external region of the cylinder with saline solution, thus imposing the reference potential at infinity.

This assumption is justified by the significantly larger radius of such a cylinder with respect to the dimension of the nerve fascicles. Different approaches for implementing the FEM model have been attempted. Macroscale models developed in literature used the FEM simulation software Comsol Multiphysics, but other FEM modeling environments can be considered, such as FEniCS or Ansys [101, 102]. A peripheral nerves simulator (PyPNS) was recently developed in Python by Lubba et al. [103]. In this computational model unmyelinated and myelinated fibers are considered. To describe their electrical dynamics the HH model and the MRG axon model were used respectively. The electric potential is extracted from FEM simulations, assigning different tissue properties in a similar way to that treated above, and is imported into the python simulator to study axons activation. In this work the following assumptions are considered: the axon behavior is not dependent on the other fiber close to it; properties related to the type of ion channels and geometry of axons are fixed; quasi-static approximation of Maxwell's equations is applied to the space that surrounds the fibers; the assumption of purely resistive media is considered for all the tissues. As in [103], to reduce computational time, the electric potential is precomputed in the FEM model and imported in PyPNS. The FEM model has specific settings,

Table 2: Summary of main features of the mathematical models.

	McNeal	SENN	Sweeney	mSENN	MRG
Equivalent electric circuit	Single cable	Single cable	Single cable	Single cable	Double cable
number of Nodes of Ranvier	11,21,31.	91	19 compartments	10,20,25,60	21
myelin sheath	perfect insulator	perfect insulator	perfect insulator	perfect insulator	explicit representation
dynamics	F-H non linear equations only in the excitation node	F-H non linear equations on all the nodes of Ranvier	Sweeney equations on all the nodes of Ranvier	like SENN	MRG equations on all the nodes of Ranvier
body temperature	20 °C	20 °C	37 °C	37 °C	37 °C
fiber diameter	20µm	20µm	10µm	10µm	9 values from 5.7 to 16 µm
model based on studies of	frog	frog	rabbit	frog	human, rat, cat

and is based on a simplified circular symmetric geometry, including axons and epineurium, and the properties of saline solution for the environment surrounding the nerve model are also considered.
There exist works that study not only the electrical stimulation of axons but also other types of peripheral nerves stimulation. A recent work [104] studied magnetic neural stimulation using computational models. To forecast the stimulation thresholds of in vivo magnetic stimulation of rat sciatic nerve and to compute the electric fields induced by the magnetic stimulation, a multiresolution impedance method coupled with the Frankenhauser-Huxley axon model to study the fiber activation according to the related membrane dynamic properties has been produced. The work takes into account the effects of fascicles and axons location and their electrical properties, which play an important role in the predicting of induced electric fields.

2.5 DISCUSSION

Knowing the type of ion channels that can be found on peripheral nerve fibers is important for researchers working in the framework of computational models of electrical nerve stimulation. In fact, according to the animal model and the type of nerve fibers to be studied, specific settings of ion channels can be modeled. In the previous sections, the most used mathematical models of nerve fibers and ion channels membrane potential dynamics in mammalians and humans have been treated. The aforementioned computational models are compared to pave the way for new researches on neuroprosthesis multiscale simulation. Aspects related to computational cost should be considered in both neuronal and FEM modeling. It is evident that

the main aspects influencing computational cost, a part the characteristics of the machine used to implement the simulations, are the adopted geometry of the nerves and the temporal resolution of the numerical approximation of equations.
In Section 2.3 on mathematical models of axons, two different types of equivalent electric circuits are considered: a single cable model and a double cable model. In all the analyzed mathematical models that used the single cable model, the axons myelin sheath is considered a perfect insulator, so, in the equivalent electric circuit, it is modeled as a high-value resistance. On the other hand, the double cable model used in the MRG work considers an explicit representation of the myelin sheath and also other sections between two consecutive nodes of Ranvier. In particular, internodal and paranodal sections are considered. Each mathematical model treated could be used to describe the nerve fibers dynamics when it is subjected to a current stimulus, accounting that as specified in Table 2 some models are validated only on data from amphybian, i.e. McNeal, SENN and mSENN models. For studies related to our interests, with the clinical application in human upper limb prosthetics, a mathematical model of axon with explicit representation of myelin sheath, to describe median nerve fibers is needed. Hence, it is possible to affirm that according to experimental validation of these studies and the equivalent electric circuit consideration, the MRG model can be more realistic to represent human axons.
Ion channels treated in the original microscale models can be considered, or they can be modified according to the nerve fibers that researchers want to study, also considering other ion channels if needed. The number of nodes of Ranvier and, accordingly, the length of the axon considered in the computational model depend on the boundary condition that has to be set and on the morphology of the real fiber to be studied. In all the models, the condition is that the membrane potential is zero at the boundary. According to the used parameters, the number of nodes can be selected. In the models analyzed, different numbers of nodes are used, as shown in Table 2. According to the considered model, the electrical properties of the equivalent circuit of the nodes are different. The computational models used different equations to describe the dynamics in nodes of Ranvier. The MRG model is based on parameters from human, rat, and cat data. It describes mammalian experimental data, so it is the model more suitable for human fibers compared to the other models that are based on amphibian or rabbit (no potassium channels) data.

The fiber diameters considered in the models are in the range from 10 to 20 μm. All these diameters can be considered for human fibers, so the choice of the fiber diameter has to be done according to the anatomical properties to be modeled. The described models are also different in considering the body temperature in the descrip-

tion. Sweeney, mSENN, and MRG models used body temperature of mammalian.

2.6 CONCLUSIONS

In this chapter, a multiscale approach to neural cell stimulation has been discussed. The first part (Section 2.2) deals with the physiology of neural cells in different animal models, starting from mammals to get to humans. The second part (Section 2.3) deals with mathematical models of neural cells considered in the literature for describing their behavior. In particular, the elements to be considered to build an axon model are treated, from unmyelinated nerve fiber discarding temperature dependence, up to a double-cable axon model including nodal and internodal sections surrounded by myelin sheet, and temperature feedback. The third part deals with the combination between microscale mathematical models and macroscale FEM models, taking into account anatomical tissues and electrodes features or other devices stimulation properties.

This study can be useful to develop new multiscale studies on neural cell stimulation, taking into account different types of ion channels according to the physiology of nerve cells and to the specific stimulation techniques, with the aim of defining a comprehensive mathematical model for *in silico* experiments. Indeed, such a framework can be easily generalized to include other stimulating techniques, such as focused ultrasound stimulation or transcutaneous electrical nerve stimulation.

In conclusion, the use of computational modeling is a very helpful instrument to study nerve fibers stimulation techniques. Thanks to these models, it is possible to obtain quantitative results about the behavior of the tissues subject to external stimuli, then the results can be used to forecast the experimental outcomes. If needed, it is possible to modify the experimental conditions or otherwise to design stimulation devices according to the simulation results.

3

SIMULATION STUDIES ON INTRANEURAL ELECTRICAL STIMULATION OF HUMAN MEDIAN NERVE

3.1 INTRODUCTION

In the research field of upper limb prosthesis, the restoration of sensory feedback is fundamental to interact with the environment. The electrical neural stimulation of peripheral nerve is the technique that more than the others allows to restore sensory feedback eliciting sensations similar to the natural ones [10–12]. In order to electrically stimulate the nerves to restore sensory feedback, different interfaces were developed, such as intraneural or cuff electrodes and flat interfaces. Due to the high invasiveness of the neural solution, it is fundamental to preliminary study the nerve-electrode interaction by means of computational simulations. From the simulation results, optimal stimulation parameters and location of the electrode into the nerve can be derived, to obtain a better fiber recruitment related to the tactile sensation to be provided to the amputees. The study of stimulation parameters and electrode implant properties from a computational framework can be a useful support guide to the experimental tests and can lead to design new generation of electrodes and novel interfaces suitable for restoring sensory feedback. The study of neuroprosthetic devices and stimulation techniques through a computational framework is a useful method to set stimulation parameters and to study the interaction between nerve tissue and electrode, as demonstrated in recent papers [3, 18, 21]. Several works deal with multiscale computational approach to study the nerve-electrode interaction, coupling the results from a Finite Element Model simulation and from computational axon or neuron model.

In the study of Shiraz et al. [18], a computational multiscale method was used to study the pudendal nerve stimulation, different kind of stimulators, electrodes and tissues were considered, according to the location of the pudendal nerve. In [15], a similar problem is considered: different kind of electrodes, Transverse Intrafascicular Multichannel Electrode (TIME) model and Flat Interface Nerve Electrode (FINE) model, are used. The study treated the selectivity of these kind of electrodes using a fixed stimulus waveform.

Another aspect related to the computing time needed to obtain the solution of the FEM model is important to study. In the work of Romeni et al. [105] a review study is presented, focusing the attention on the different steps followed to build a complete hybrid

model, defined as the combined results obtained from FEM and Neuron models. One possibility related to the design of the nerve model is the simplification of the nerve section geometry to decrease the computational time related to the meshing and the solution computing. Starting from the segmentation of histological images fascicles of different shape can be found. The approximation of the inner fascicle to simpler geometrical shape of circles or ellipses can be a possible choice to reduce meshing and computational time.

PROGRESS BEYOND THE SOA Our contribution in this chapter is to propose computational models to study the behaviour of a 3D model of human median nerve subjected to a direct current stimulation by mean of the intraneural electrode model ds-FILE. The approach used include the coupling between the results obtained by FEM in Comsol with the mathematical model of axon in Neuron software [106]. A realistic computational model, using FEM, of the human median nerve and of the ds-FILE intraneural electrode is introduced [107]. This type of electrode is different from the electrodes used in [15]. In particular, its geometrical properties and active sites shape are different from the ones of the TIME model; furthermore, since it is an intraneural electrode, it has different characteristics with respect to the FINE model. The ds-FILE electrode has been already used in experiments on human amputees [7], making it particularly interesting for future comparison between the results obtained in simulation and the experimental ones. A first comparison between simulations and experimental results on human amputee will be discussed in the second part of Chapter 4. The other aspect related to the possibility to reduce computational time of the FEM simulation will be discussed in Section 3.3. The 3D model of human median nerve is developed considering a faithful anatomical reconstruction of the nerve section and a simplified nerve section approximating inner fascicles from polygonal to elliptical shape. The comparison of the electric potential results will be studied to quantify the goodness of the approximation.

CHAPTER 3 IS STRUCTURED AS FOLLOWS: In Section 3.2, three types of stimuli discussed in [1] will be treated and compared. The study of the nerve fibers activation subjected to a current stimuli, at a fixed distance from an active site will be treated. The stimulus waveform and the current level required to excite a population of nerve fibers in the target nerve are modelled. In the same way, fibers activation in cutaneous and muscular fascicles, keeping the location of the electrode fixed, is studied. In particular, focusing on the possible stimulation of muscular fascicle related to *flexor digitorum superficialis* when active sites of the electrode are inside a terminal cutaneous fascicle close to it is an important issue that, to our knowledge, is still not covered by the literature. Further, to study the fibers activation,

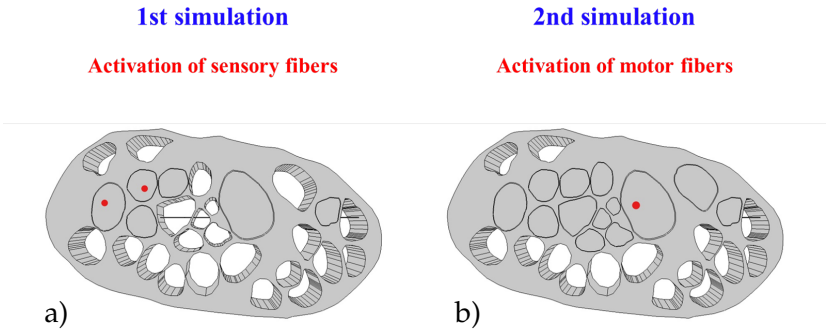

Figure 5: 3D FEM model of human median nerve related to the two simulations. a) Nerve fascicle with red spots related to sensory fibers; b) nerve fascicle with red spot related to muscular fascicle. They are considered to study electric potential distribution on axon fibers along the nerve, for ten distances from the active site.

ten different distances from the electrode are considered in each fascicle. The three types of waveform used are the safest as reported in literature [1].

The goal of the Section 3.2 is to discuss fibers activation properties subjected to three different stimulus waveform at a fixed distance from an active site in a nerve fascicle and to study nerve fibers activation subjected to the same stimuli at different distances from the active site in two cutaneous and one muscular fascicles.

Regarding to the second case study, active sites of the electrode were positioned in a terminal cutaneous fascicle with sensory fibers in the inner of it, the other fascicle was close to this one (Figure 5 a) and the fascicle related to the *flexor digitorum superficialis* was at a certain distance from the terminal cutaneous fascicles, as shown in Figure 5 b. For each fascicle ten different distances from the electrode were tested.

As discussed in Chapter 2, Section 2.3.7 and Section 2.4, the MRG axon model [83] is a useful axon model to represent axon fibers of peripheral median nerve, representing them in more realistc way, considering different sections of the axon and myelin sheath. So it is used to evaluate the nerve fibers activation and recruitment. On the basis of the results, conclusions can be drawn on how axon fibers located at different distances from the active sites in a nerve fascicle and in a fascicle close to it are activated, as a function of type of waveform signal and current amplitude.

In Section 3.3 of this chapter 3D models of human median nerve are developed. Two different geometries of inner fascicles shape are considered: anatomical geometry and simplified geometry. The anatomical geometry is developed starting from the segmentation of the histological image of a human median nerve section. The simplified geometry is obtained from the same image and approximating the shape of the inner fascicles to ellipses.

The goal of the Section 3.3 is to compare the electric potential distributions into the median nerve subject to a current stimulus via FEM models, using anatomical and simplified geometry of inner fascicles. The advantage is that if the two distributions are similar, it is possible to approximate the anatomical geometry with a simplified one obtaining the reliability of results and less computational time to mesh and solve the FEM model. To gain more insight into the current intensity necessary to activate nerve fibers, the percentage of activation (PA) of the axons into the fascicles is also studied.

3.2 Analysis of stimulation waveform and electric potential in cutaneous and muscular fascicles

3.2.1 *Methods*

In order to obtain a realistic simulation of a human median nerve, a Finite Element Method model is built considering nerve anatomical properties. A current stimulus from the intraneural electrode is delivered to the nerve model and the electric potential distribution into the nerve is studied. After an interpolation of electric potential values on different sections of the axon fiber, the activation of the fibers is studied. Electric potential is used as external potential in an axon model built in Neuron software [106]. The activation of the axons is evaluated by the generation of the action potential on the first and last node of Ranvier of the axon fiber. In the next subsections, a detailed description of the Finite Element Method model of the interaction between the electrode and the nerve and a description of the used axon model are provided.

3.2.1.1 *Finite Element Model for Nerve and Electrode*

To obtain a realistic human median nerve model, image data from the histological section of the human median nerve [108] are analysed (Figure 6 a). The image is segmented using the software imageJ (Figure 6 b), and the obtained geometry is imported in COMSOL Multiphysics v5.3 ®(COMSOL, Ltd, Cambridge UK) and extruded along the longitudinal axis to build a 3D geometry (Figure 6c). The nerve model is segmented in three different tissue classes: epineurium, perineurium, endoneurium. On the basis of the literature [15], the values of conductivity are set as follows. Anisotropic conductivity tensor is assigned to endoneurium, with longitudinal value of 0.571 S/m and transverse value of 0.0826 S/m. The epineurium and perineurium are assumed isotropic media with a conductivity of 0.0826 S/m and 0.00088 S/m respectively. The electrical conductivity related to the different tissues are shown in Table 3 . A homogeneous medium of saline solution simulates the intraoperative environment.

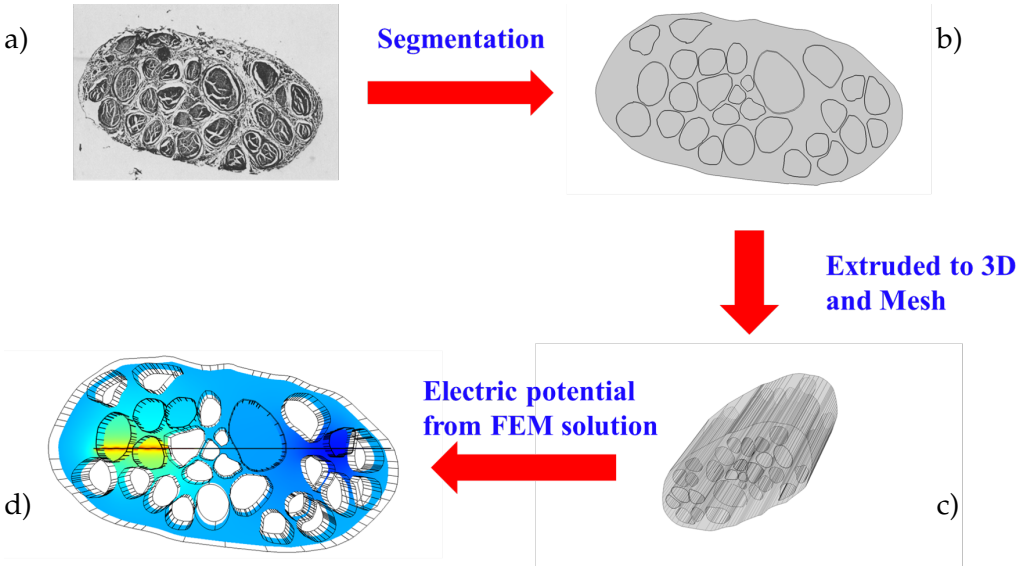

Figure 6: Scheme of the Finite Element Method model of the nerve fiber-electrode interaction

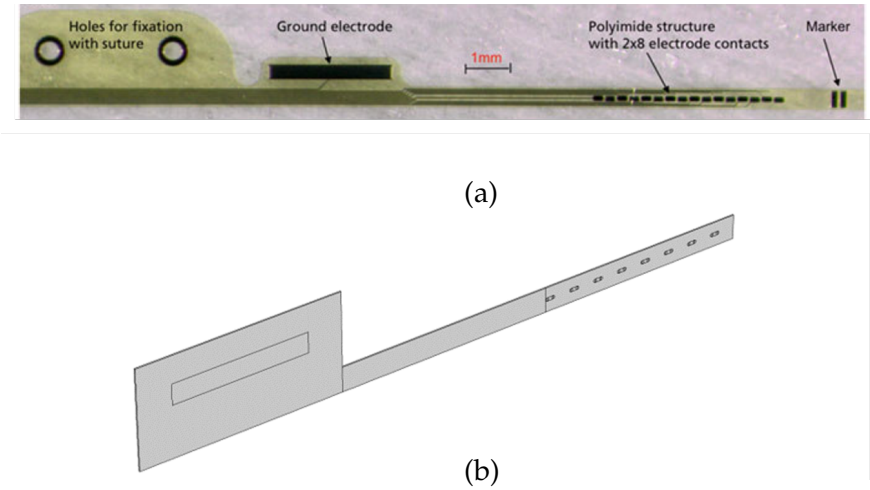

Figure 7: ds-FILE electrode (a); CAD model of the ds-FILE electrode (b).

Table 3: Electrical conductivity related to different tissues

Tissue	Conductivity (S/m)	Reference
Endoneurium	0.571	[15]
	0.0826	
Epineurium	0.0826	[15]
Perineurium	0.00088	[15]

A Dirichlet boundary condition is set at the outer surface of the cylinder (saline solution). A quasi-static approximation of the Maxwell's equations [100] is considered as shown in the following equation

$$\nabla \cdot (\sigma \nabla V) = 0 \tag{13}$$

where σ and V are the conductivity of the medium and the electric potential respectively. The model was implemented in COMSOL Multiphysics, using the AC/DC module, Electric Currents physics in Stationary setting. COMSOL Multiphysics allows to solve the following Maxwell's equations

$$\nabla \cdot \vec{J} = Q_j \tag{14}$$

$$\vec{J} = \sigma \vec{E} + \vec{J_e} \tag{15}$$

$$\vec{E} = -\nabla V \tag{16}$$

where $\vec{J}$, Q_j, $\vec{E}$ and $\vec{J_e}$ are the current density, the current source, the electric field and the external current density respectively. Q_j and J_e are setted to zero everywhere in the model and the Maxwell's equations were solved in quasi static approximation.

The differential equations are solved using finite element methods, Figure 6 d. The radius of the external cylinder is set at 38 mm that is larger than the dimension of the human median nerve [109]. This would implement the approximation of the ground at infinity.

The electrode geometry is built in Comsol ®(Figure 7) and the ds-FILE electrode is modeled as a polymide structure with 20 µm thickness and 360 µm height. Sixteen active sites are considered according to the ds-FILE properties [7]. The conductivity of polymide is $6.7 \cdot 10^{-14}$ S/m and of active sites is $8.9 \cdot 10^{6}$ S/m. The electrode is placed trasversally at half height of the nerve model.
The current amplitude is set to 10 µA, which is an arbitrary level to be scaled at subsequent stages.

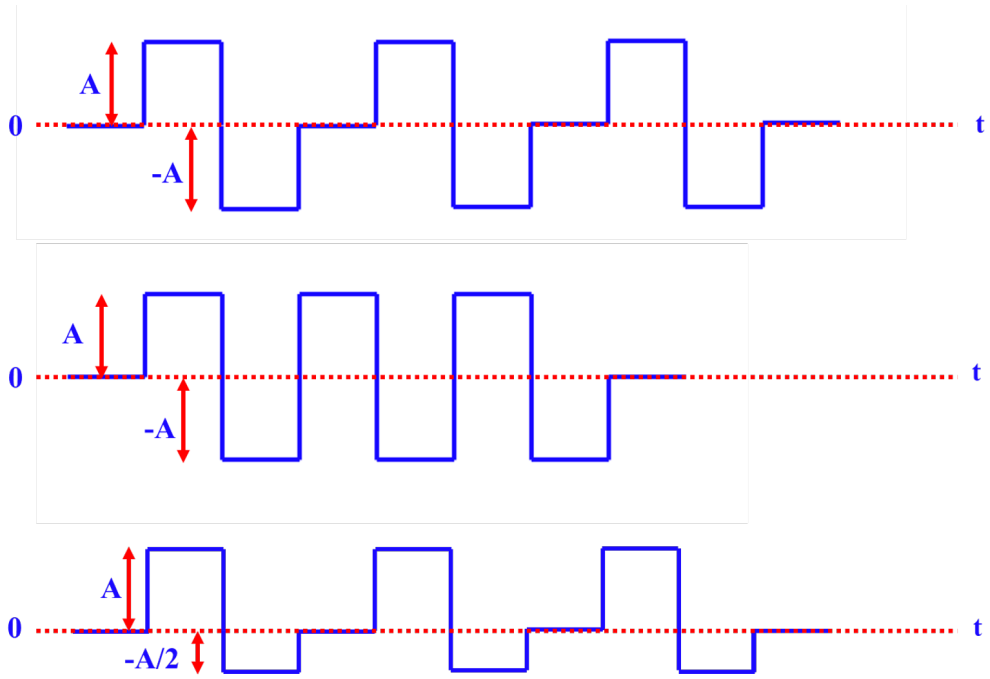

Figure 8: Three different types of stimulus waveform. i) biphasic charge balanced stimulus with inter-pulse delay, ii) biphasic charge balanced stimulus without inter-pulse delay, iii) biphasic charge unbalanced stimulus with inter-pulse delay. Time duration of pulses and inter-pulse delay is 80 µs

Two simulations are performed. From the first simulation, a nerve fascicle with active sites of the electrode implanted into it is considered. The electrical potential distribution into the target fascicle and in a nerve fascicle close to it is studied (Figure 5). These fascicles correspond to sensory fibers according to [108]. In this simulation some fascicles far from the target fascicle are excluded from the computing to optimize it.

From the second simulation electric potential distribution into a fascicle, that according to literature could be related to motor fibers, are studied. According to studies of Jabaley [108], the electric potential distribution into the fascicle named *Flexor Digitorum Superficialis* is considered. The electrode position is the same of the first simulation Figure 5.

Also other fascicles are included compared to the previous simulation, to understand how other fascicles affect the potential distribution into the nerve.

3.2.1.2 *Median nerve axon model*

A double layer cable model of myelinated fibers in the median nerve is developed to detect nerve fibers activation. The axon model is considered with imperfect insulation and implementing McIntyre-

Richardson-Grill channel mechanisms for the nodes of Ranvier [83]. Compartments between two nodes are made of two myelin compartments, two paranodal and ten internodal [18]. As reported in McIntyre et al. [83], the electrical behaviour of the axon is represented by the model using linear and non linear membrane dynamics. The nodes are described by two different sodium conductances (non linear fast sodium and persistent sodium), a slow potassium conductance, a linear leakage conductance and the membrane capacitance.

The equations that describe ion currents, rate constants and time changes of gating parameters are expressed in the following equations.

Fast sodium current, the rate constants related to it and time change of gating parameters

$$I_{Naf} = g_{Naf} m^3 h (V_m - E_{Na}) \tag{17}$$

$$\alpha_m = \frac{6.57(V_m + 20.4mV)}{1 - e^{-(V_m+20.4mV)/10.3mV}}$$

$$\beta_m = \frac{-0.304(V_m + 25.7mV)}{1 - e^{(V_m+25.7mV)/9.16mV}}$$

$$\frac{dm}{dt} = \alpha_m(1 - m) - \beta_m m \tag{18}$$

$$\alpha_h = \frac{-0.34(V_m + 114mV)}{1 - e^{(V_m+114mV)/11mV}}$$

$$\beta_h = \frac{12.6}{1 + e^{-(V_m+31.8mV)/13.4mV}}$$

$$\frac{dh}{dt} = \alpha_h(1 - h) - \beta_h h \tag{19}$$

Persistent sodium current, the expression of its rate constants and the time change of the gating parameter:

$$I_{Nap} = g_{Nap} p^3 (V_m - E_{Na}) \tag{20}$$

$$\alpha_p = \frac{0.0353(V_m + 27mV)}{1 - e^{-(V_m+27mV)/10.2mV}}$$

$$\beta_p = \frac{-0.000883(V_m + 34mV)}{1 - e^{(V_m+34mV)/10mV}}$$

$$\frac{dp}{dt} = \alpha_p(1 - p) - \beta_p p \tag{21}$$

The slow potassium current, its rate constants and the time change of the gating parameter are expressed as follows:

$$I_{Ks} = g_{Ks} s (V_m - E_K) \tag{22}$$

$$\alpha_s = \frac{0.3}{1 + e^{-(V_m + 53mV)/5mV}}$$

$$\beta_s = \frac{0.03}{1 + e^{-(V_m + 90mV)/1mV}}$$

$$\frac{ds}{dt} = \alpha_s (1 - s) - \beta_s s \tag{23}$$

The leakage current can be expressed in the following equation

$$I_{Lk} = g_{Lk} (V_m - E_{Lk}) \tag{24}$$

As cited in [83], the dynamics is related to specific experimental studies [34, 35, 92].

Fiber diameters follow two Gaussian distributions with mean of 4 and 12 and standard deviation of 1.5 and 1 respectively [15, 110], myelinated nerve fibers fall in two classical groups, the smaller Aδ and the larger Aα groups of fibers. Geometrical properties are derived interpolating experimental data from [83]. The first node of Ranvier is randomly placed between 0 and Δx of the arclength of the nerve fiber, Figure 9; note that Δx is defined as node to node distance for a fiber. Compartments are inserted between two nodes of Ranvier along the fiber and the model is ended by a node [18].
This procedure is repeated for 100 fibers in the nerve as studied in [18]. A fiber is considered activated when the action potential propagate it along all the fiber length. The percentage of activation (PA) of fibers, defined as the number of activated fibers out of 100, is calculated. Models are imported in Neuron v7.4 to solve the differential equations using the Backward Euler integration method with 0.005 ms steps. Electrical potential along the nerve is solved in Comsol ®, interpolated in Matlab ®and imported as extracellular potential in Neuron. Extracellular potential is pulsed, with three pulses. The procedure is summarized in Figure 10 .

Three different types of stimuli waveform are considered (Figure 8): i) biphasic charge balanced pulses of 80µs with inter-pulse delay of the same duration, ii) biphasic charge balanced pulses of 80µs duration without an inter-pulse delay and iii) biphasic charge unbalanced pulses of 80 µs duration with inter-pulse delay of the same duration. Under quasi-static approximation, to simulate different current amplitude values are multiplied. The percentage of activation of the fibers is measured for the three types of stimuli, the stimulus (i) is the same as described in [7]. The three stimuli that are considered are already proven in the literature as safe and effective as reported in Figure 9 of [1] in terms of *effective action potential initiation, tissue damage and corrosion of electrode materials*.

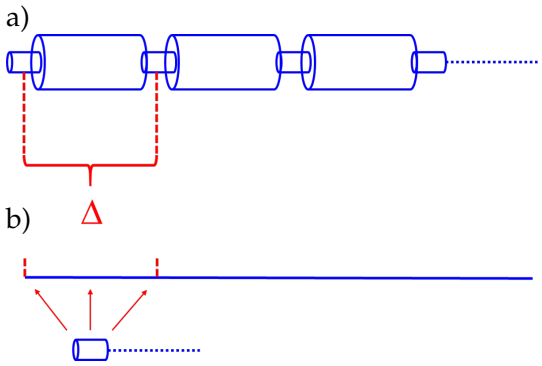

Figure 9: Schematic representation of the axon model. (a) The axon divided in different compartments: node of Ranvier (small cylinder) and myelin, paranodal and internodal sections (big cylinder). The distance between two nodes of Ranvier is defined as Δ. (b) The first node of Ranvier of the axon is randomly placed between 0 and Δ along the arclength of the nerve fiber, represented as the blue solid line .

3.2.2 *Results*

In this section the data related to the Percentage of Activation in human median nerve fibers as the current stimulus amplitude changes are reported for the three different types of stimuli waveforms shown in Figure 8 .

Data are related in a fascicle within the active site of the electrode at a fixed distance from the electrode, and muscular and muscular fascicles at different distances from the electrode Figure 5 .

The PA in % vs current intensity is shown in Figure 11, Figure 12, Figure 13 for each of the three stimulus waveforms, at a fixed distance from the electrode into the first sensory fascicle from left side in Figure 5. The simulation is performed by varying the current amplitude for each stimulus waveform. The current amplitude is in the range from 50 to 160 µA. This current amplitude range is found experimentally, starting from an arbitrary current amplitude the value is varied looking for the activation threshold and the value of total activation that corresponds to the PA=100%. To evaluate the PA, three consecutive pulses are considered. The fibers subjected to the biphasic charge balanced waveform with interpulse delay are activated starting from a current amplitude of 80 µA and PA=100% at a current amplitude of 110µA Figure 11.

As shown in Figure 12, axon fibers require 120 µA current to generate an action potential and PA=100% when the current amplitude reached 150 µA.

Considering the third type of stimulus waveform shown in Figure 8 and the corresponding fiber activation in Figure 13, it is possible to note that fibers are activated at 75 µA and PA=100% at a current value of 95 µA.

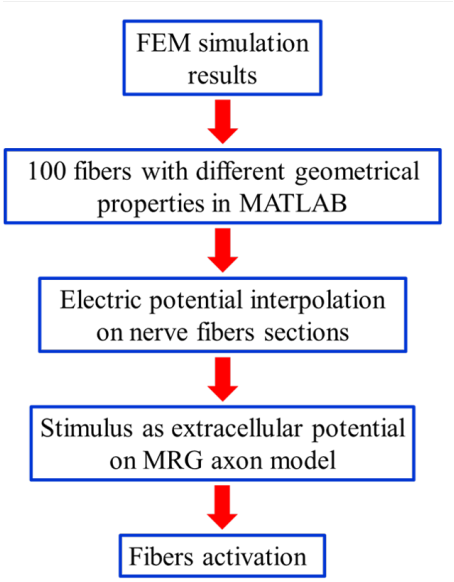

Figure 10: Schematic view of the procedure used to process simulation data

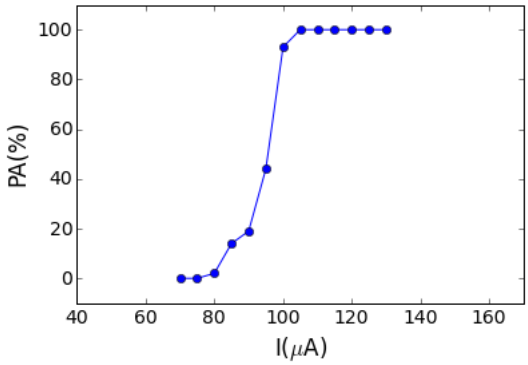

Figure 11: PA of the fibers *vs* current stimulus amplitude, for the i) signal in Figure 8

Data related to the percentage of activation of human median nerve fibers in different fascicles Figure 5 as the current stimulus change are reported for the three different types of stimulus waveform.

The PA is studied for ten distances from the active site in the first target fascicle shown in Figure 14 a).

The PA versus current intensity is reported in Figure 14 e), f), g) for the three different stimulation waveforms and for ten distances from the active site. Simulation were performed varying the current amplitude of the three different stimulus waveforms. From Figure 14 e, related to the biphasic charge balanced stimulus with inter-pulse delay, it is possible to observe that the current amplitude to activate axon fibers is in the range between 65 to 100 μA for all the distances from the considered active site. From Figure 14 f and Figure 14 g, it is shown that the current amplitude to activate axon fibers is in the

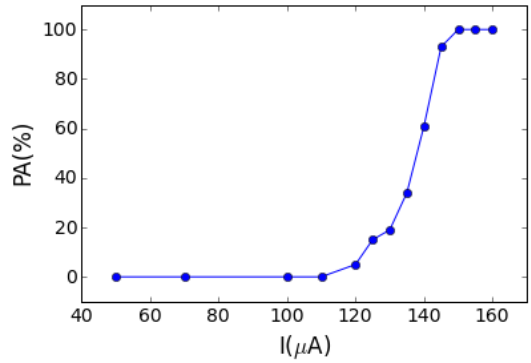

Figure 12: PA of the fibers *vs* current stimulus amplitude, for the ii) signal in Figure 8

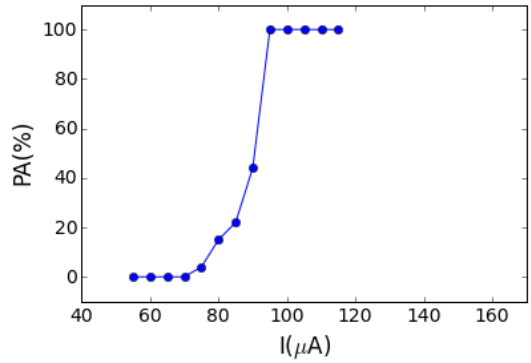

Figure 13: PA of the fibers *vs* current stimulus amplitude, for the iii) signal in Figure 8

range 95 to 145 µA and 60 to 95 µA, respectively. The corresponding waveform stimuli are the charge balanced stimulus without interpulse delay and the charge unbalanced stimulus.

The current amplitude ranges are found experimentally, starting from an arbitrary current amplitude value of 50 µA. For the PA evaluation three consecutive pulses are considered. Considering the ten distances from the active site from which the electrical potential distribution is evaluated, they are along all the course of the nerve. The first distance is close to the active site, other distances are 100 µm each from the other so the first is around some microns far to the active site and the last is 1 mm from the active site. All the distributions are in a nerve fascicle where the active site is implanted in. According to literature, this fascicle could be related to sensory fibers. In Figure 15, the current amplitude necessary to obtain in the range 95%-100% of activated fibers for three different waveforms as the distance from the active site change is shown.

In Figure 16 e, f, g the percentage of activation as the current amplitude changes for the different waveforms are considered. The target fascicle considered is the second fascicle shown in Figure 16 a, the first distance considered is the lowest one in Figure 16 a close to the electrode and the other distances are 100 µm apart from each other.

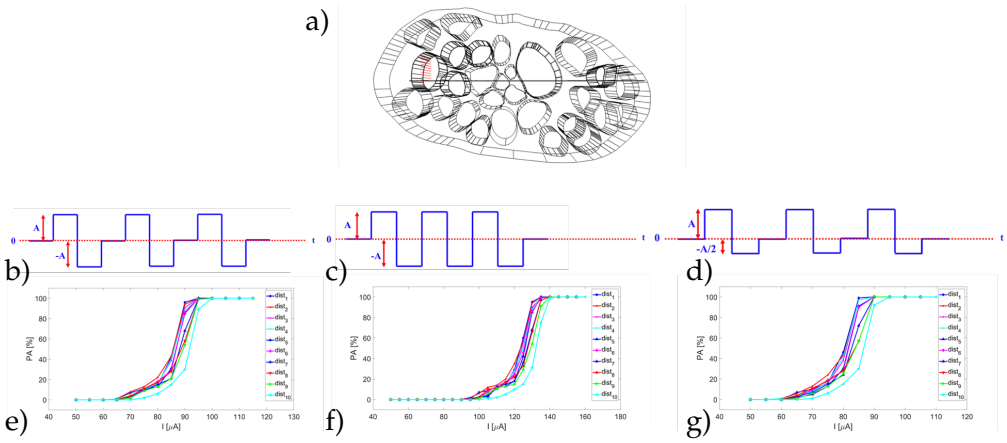

Figure 14: a) 3D scheme of the target fascicle as shown in Figure 5: red lines highlight ten distances considered from the electrode in the fascicle. Three different types of stimulus waveform: b) biphasic charge balanced stimulus with inter-pulse delay, c) biphasic charge balanced stimulus without inter-pulse delay, d) biphasic charge unbalanced stimulus with inter-pulse delay. Time duration of pulses and inter-pulse delay is 80 µs. e),f),g) Percentage of activation vs current amplitude, for the corresponding stimulus waveform (b), c), d), respectively), for ten different distances from the active site in the same fascicle.

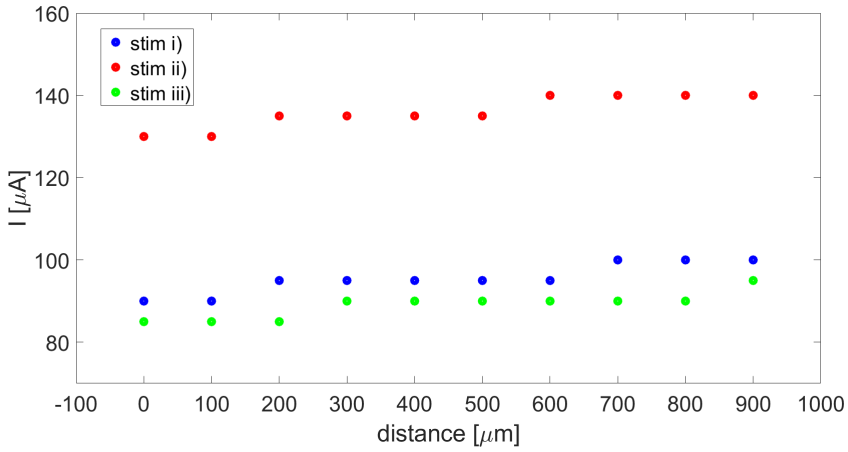

Figure 15: Current amplitude to obtain a 95% < PA < 100% vs distance from the active site, for three different stimulus waveform shown in Figure 14.

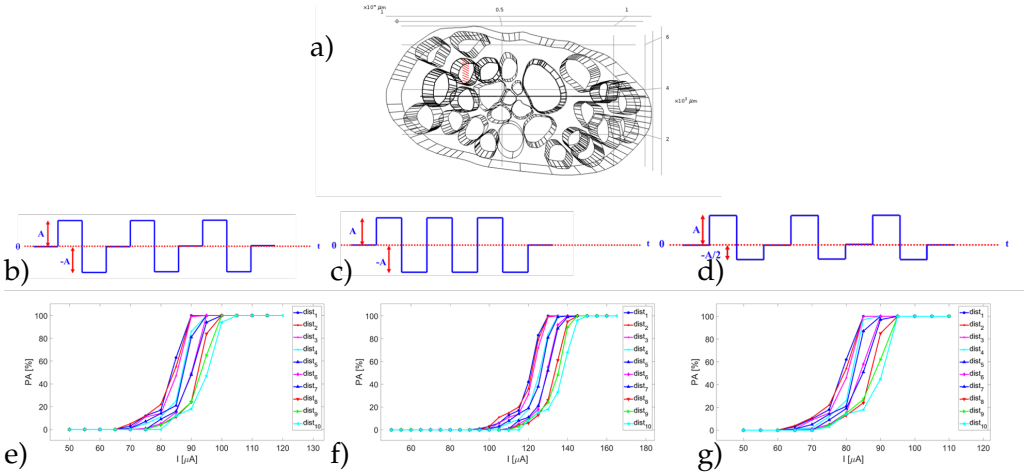

Figure 16: a) 3D scheme of the target fascicle as shown in Figure 5: red lines highlight ten distances considered from the electrode in the fascicle. Three different types of stimulus waveform: b) biphasic charge balanced stimulus with inter-pulse delay, c) biphasic charge balanced stimulus without inter-pulse delay, d) biphasic charge unbalanced stimulus with inter-pulse delay. Time duration of pulses and inter-pulse delay is 80 μs. e),f),g) Percentage of activation vs current amplitude, for the corresponding stimulus waveform (b), c), d), respectively), for ten different distances from the active site in the same fascicle.

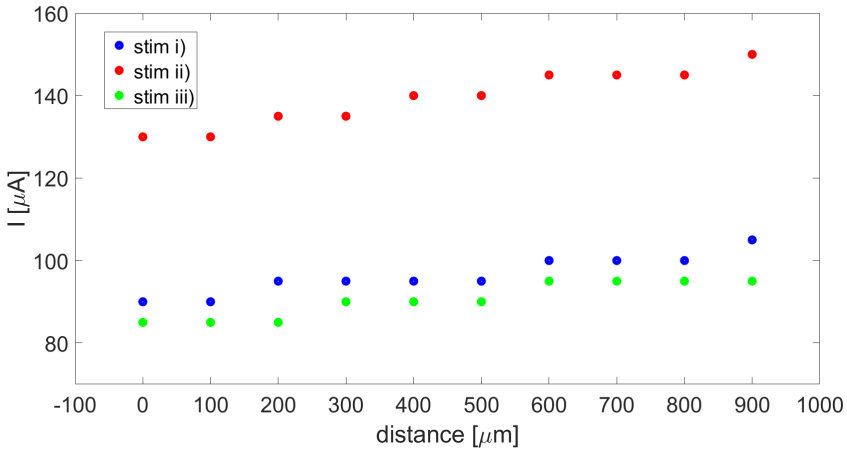

Figure 17: Current amplitude to obtain a 95% < PA < 100% vs distance from the active site in the second fascicle, for ten different distances.

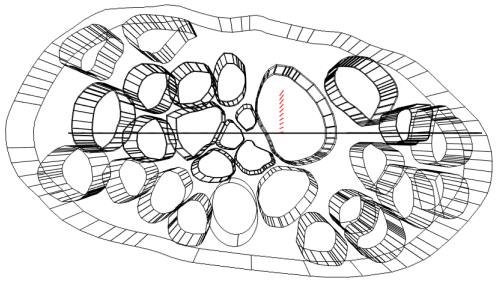

Figure 18: 3D scheme of the muscular fascicle. The red lines highlight ten distances from the electrode

For such fascicle, the PA vs current amplitude was analogously studied. Results related to the fibers subjected to the i) stimulus waveform are shown in Figure 16 e, it is possible to note that starting from a current amplitude of 70 µA axon fibers are activated and a PA=100% is reached at 110 µA. Results shown in Figure 16 e, f are related to waveform signal ii) and iii) . Axon fibers are activated starting from 95 µA and 65 µA and the PA=100% is reached at a current amplitude value of 150 µA and 110 µA, respectively. The minimum current amplitude to obtain a 95% - 100% of activation for three different waveforms is shown in Figure 17.

No plots are shown about the simulation related to axon fibers in muscular fascicle shown in Figure 18. From the simulation, it was found that the current amplitude necessary to activate the axon fibers in the muscular fascicle, when the stimulus is applied into cutaneous fascicle is one order of magnitude higher than the current amplitude used to activate fibers in the fascicles shown above. This result can be related to the shielding of other fascicles and tissues.

3.2.3 *Discussion*

Computational FEM-Neuron hybrid models can be useful to design novel neural interfaces in the research field of upper limb prostheses. The same approach can be used to develop new modalities for restoring sensory feedback in upper limb amputees. A computational simulation allows to study electrical potential distribution into nerve fascicles subjected to an electrical current stimulus through an intraneural electrode. The activation can be studied using an axon model built in Neuron. Knowing the activation properties is an important element to evaluate the efficacy of the neural stimulation. Therefore, the percentage of activation for three different stimulus waveform by varying the stimulus intensity and the distance between the electrode and the possible location of an axon fiber is studied.

In Figure 11, Figure 12, Figure 13 it can be observed that the increase of current intensity lead to an increase of percentage of activation of nerve fibers. The trend is the same for the three types of

stimulus waveforms even if the threshold value to reach PA=100% is quite different. From Figure 11 ,Figure 12, Figure 13 it is possible to note that the threshold to activate 100% of the fibers is lower in case of the third stimulus waveform (i.e. biphasic charge unbalanced stimulus with inter-pulse delay) and it is higher for the biphasic charge balanced ones.

The reason could be related to the sign of the stimulus and its time duration. To activate a neural cell, it is necessary to depolarize the membrane: if the depolarization is above a threshold, an action potential fires. The third waveform requires a lower value of threshold to activate axon fibers compared with the other stimuli. The reason could be related to the time that the stimulus spends in a positive state. In this case, the stimulus spends the same time of the stimulus i) in a positive state and in the o state, but even if the time in a negative state is the same, in this case the absolute value of the current intensity is lower than the absolute value of the first case.

The first waveform requires a higher value of threshold to activate all the fibers because the time that the stimulus spends in a positive state and in a zero state is the same to the case iii) but the absolute value of the current amplitude in the negative state is higher than the case iii).

The second type of waveform has a time duration lower compared to the others, so the signal spends less time in a positive state compared to the other stimuli and to the time duration of all the stimulus and the activation threshold is higher than the other two cases. So it is possible to adfirm that the third stimulus, that has a lower threshold of current amplitude to activate a given percentage of fibers than the others stimuli, is the safer among the three waveforms considered. Because it is possible to activate a given percentage of nerve fibers delivering lower values of currents to the tissues and accordingly reducing the possibility of tissues damaging.

Analysing the results of each stimulus waveform, it is possible to observe that the Percentage of activation related to the second stimulus increase slower than the PA related to other stimuli. It means that we can obtain a fine control on the percentage of activation of the fibers. We can also observe that the third stimulus is the safer one because it allows to stimulate a wide number of fibers giving lower current amplitudes than the values considered in the other stimuli treated in this study.

In Figure 14, Figure 15, Figure 16, it can be observed that the increase of current amplitude lead to an increase of percentage of activation of nerve fibers. They have the same trend for the three type of stimulus waveform and for both the fascicles considered. The current amplitude to activate axon fibers is different according to the signal waveform and the distance from the electrode into the considered fascicle. Regarding the fascicle in Figure 14 a, it is possible to note from

Figure 14 e-g that the current values to reach the 100% of activated fibers is different, in particular it is lower in the case of the third considered stimulus waveform and it is higher for the charge balanced ones. The same trend is observed in Figure 16 e-g related to the second sensory fascicle.
Note that, observing the percentage of activation related to each waveform, Figure 14 e-g for the first fascicle and Figure 16 e-g for the second one, the current amplitude values necessary to activate a given percentage of fibers increase according to the distance considered from the active site. Values are different according to the considered waveform.

The minimum values of current to obtain a 95% to 100% of activation, shown in Figure 15 for the first fascicle and in Figure 17 for the second fascicle, allow to note that when the distance from the active site, i.e. the source of the current, increases, an increase of current is required to activate a given percentage of axons.

A quantitative analysis has been done, showing that the safest waveform is the third one, because current values are lower than the corresponding ones for the other waveforms while the effectiveness of the stimulation is practically the same.

The reason could be related to the sign of the stimulus and its time duration. To activate a neural cell, it is necessary to depolarize the membrane: if the depolarization is above a threshold, an action potential fires.

These results can be useful to know the range of current amplitude that had to be used to activate fibers selectively in a fascicle where the active sites of the electrode are in the inner part of the fascicle or in a fascicle close to it.

Results about the muscular fascicle percentage of activation as current amplitude varies are not shown, because they are not of interest in this framework. For the application in sensory feedback restoring in upper limb neural prosthetics, the goal is to activate sensory fibers without the activation of motor fibers. So in previous sections the electrode is considered only into cutaneous fascicles. The activation of fibers in muscular fascicles is considered to know how the intraneural stimulation of cutaneous fascicles, related to sensory fascicles, can affect the activation of muscular fascicle. So in this framework the stimulation of muscular fascicles is not considered. Note that the current amplitude required to activate that nerve fibers, for all the waveforms, is one order of magnitude higher than that used to stimulate fibers close to the active site. Therefore, current values sufficient to activate sensory fibers in fascicles like those shown in Figure 5 a, cannot stimulate fibers in fascicles like those in Figure 5 b.

As shown in Section 3.1, to evaluate the possibility to reduce computational time, two other 3D human median nerve models are developed. One of the two models developed is the same treated in the

previous section, following a faithful reconsctruction of anatomical geometry surface section, the other model is considered approximating the shape of the inner fascicles to ellipsis.

3.3 COMPARISON BETWEEN ANATOMICAL AND SIMPLIFIED HUMAN MEDIAN NERVE MODELS

Two finite element 3D conductor models of the human median nerve are considered according to two different shapes of the nerve section: a model with the nerve section that has fascicles according to the anatomical geometry and a model where the fascicles shapes is approximated to simple geometrical shapes like ellipses. To obtain elliptical shapes approximations of anatomical fascicles a Matlab routine is used. Data related to anatomical fascicles are imported in Matlab and an ellipsis fitting is performed using fit_ellipse.m code by Ohad Gal [111]. Later, ellipses data are used in Comsol to build ellipses substituting the anatomical fascicles shapes. The electrical potential distributions into the median nerve due to a current stimulus provided by an intraneural electrode is analyzed. These quantities are interpolated on the compartments of the axon models in Neuron [106] to study the percentage of activation following the same procedure treated in Section 3.2.

Simulations are performed on a computer with an Intel Core i7-8750H CPU at 2.20 GHz, 16 Gb RAM.

Two sections with different fascicles shapes are obtained from the anatomical image. We refer to anatomical geometry to identify the model whose fascicles section is a faithful reconstruction of the section shape of the histological image. We refer to simplified geometry to identify the model whose fascicles section is approximated using simple geometrical shapes like ellipses. Once the two geometries of the nerve section are built, they are imported in COMSOL Multiphysics ® v5.3 (COMSOL, Ltd, Cambridge UK) in order to obtain a 3D model of 10 mm length.

Different tissues properties, (reported in Table 3) are then assigned to each of the two obtained 3D models (the one with anatomical geometry and the other one with simplified geometry) of the median nerve according to the nerve anatomy.
The electric potential distribution into the nerve model is studied solving in Comsol the equations Eq. (14),Eq. (15),Eq. (16).

FEM simulation results are coupled to the MRG axon model to study fibers activation as discussed in Section 3.2.

Stimulus waveform, defined in the extracellular potential, is a biphasic charge unbalanced waveform (the iii) stimulus in Figure 8) with the same properties. This type of waveform is considered according to results obtained in previous section (study [21]) that demonstrated its safety and efficacy compared with other types of waveforms (i.e. biphasic charge balanced with inter-pulse delay and biphasic charge balanced without inter-pulse delay).

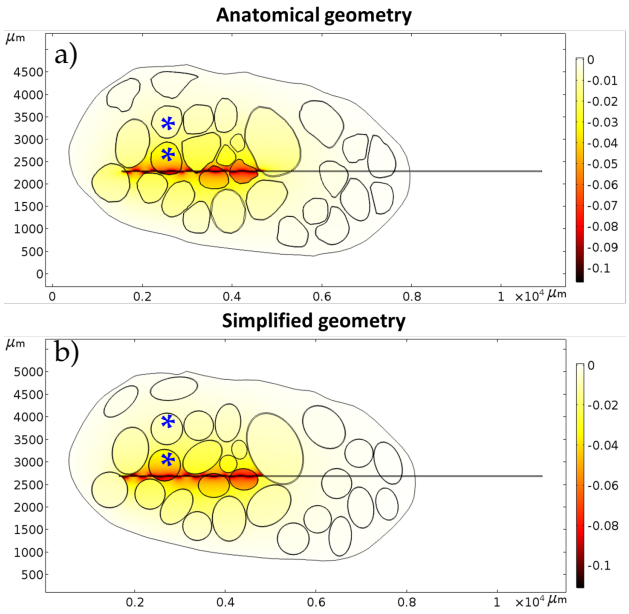

Figure 19: Color map of electric potential distribution into the human median nerve model subject to a 20µA current stimulus. a) Anatomical and b) simplified geometries of inner fascicles are shown. Fascicles with blue symbols are considered for the study. Colorbar is in Volt.

3.3.1 *Results*

In this section data related to the electric potential distribution in the median nerve model subject to a current stimulus are shown. In Figure 19 the electric potential distribution reported in a color map can be observed. Two cases are distinguished according to the shape of inner fascicles. Figure 19a and Figure 19b show the results of the simulation on anatomical and simplified geometry, respectively. These color maps were obtained setting the arbitrary current value of 20µA.

The electric potential variation, normalized with respect to the absolute value of the electric potential maximum is shown in terms of percentage of variation as a function of distance from the active site. Different simulations were performed with the two models and the obtained results are shown in Figure 20. In particular, thirteen different distances from the active site are considered: they have a distance of 100µm from each other. This distance were chosen since it is considered as the minimum one to observe a significant potential variation. The first six distances in Figure 20b (seven in Figure 20a) are in a nerve fascicle where the active site is implanted in, the remaining ones are in the fascicle near to it, along the y axis. The stimulus waveform defined in the previous section is used to study fibers activation in Neuron MRG model. In Figure 21, results related to the minimum charge quantity necessary to obtain a 100% of fibers activation, ac-

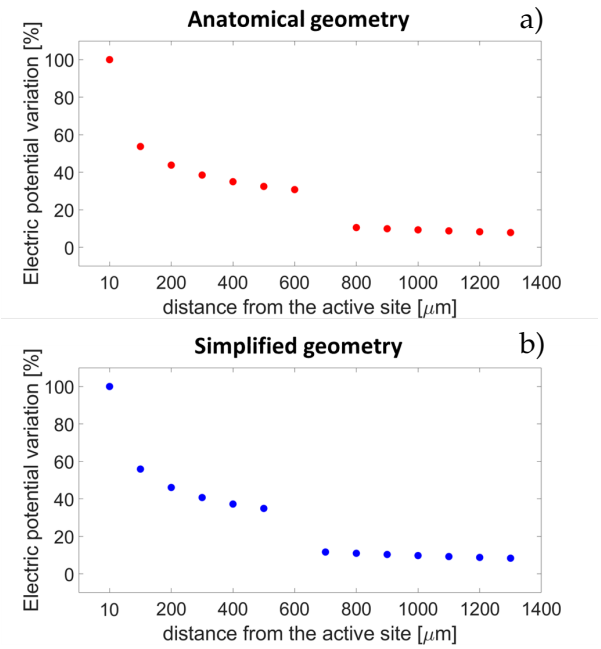

Figure 20: Electric potential variation, expressed in percentage, along the y-axis in two fascicles. The variation is considered compared to the maximum value found close to the active site of the electrode, using anatomical a) and simplified b) geometries.

cording to the MRG model, at different distances from the active site are shown.

3.3.2 *Discussion*

The complexity of the FEM geometry can affect meshing and solution computational time, so results of simulations, performed using anatomical and simplified geometry are studied and compared. In particular, computational solution time related to simplified and anatomical models are 3 minutes 43 seconds and 8 minutes 30 seconds, respectively. Other time has to be considered for the anatomical model, including the time necessary to modify the mesh when the geometrical shape is more complex. From Figure 19 it is evident that the behaviour of the fascicles is the same when a current stimulus is delivered by intraneural electrodes. The values of electric potential are in the range from -0.1 V to 0 V. From a quantitative analysis on electric potential obtained from the anatomical and simplified simulations, it is found that they follow the same trend with respect to the distance from an active site. The mean difference between the two trend is around 0.0039 V. In particular, the electric potential related to the simplified model is higher in absolute value than the anatomical one. Considering the fibers activation, it is also observed that the minimum current amplitude to obtain 100% of fibers activation using

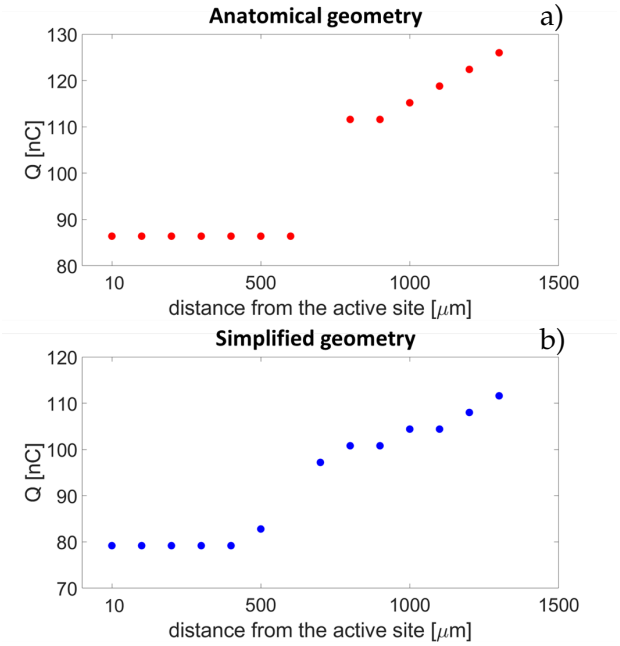

Figure 21: Electric charge necessary to activate 100% of fibers at different distances from the active site, in two fascicles, for the anatomical a) and simplified b) geometries.

the simplified model is lower of 20µA than the anatomical one. From a geometrical point of view, it is noteworthy that the area of the fascicle sections and the volume of the fascicles of the simplified model are slightly lower than the anatomical one. Considering the same current intensity and the same distances from the active site for both the models, the high (absolute) value of the electric potential in simplified model could be related to a high (absolute) value of the electric potential density.In a similar way, it could also justify the lower current amplitude necessary to activate 100% of the fibers. Considering the same current amplitude for both the models, the electric potential in the simplified model is higher than the anatomical one, so a lower current amplitude value is needed to activate 100% of fibers. The behaviour of the different tissues is similar in both the pictures, high intensity is near to the active site and the insulating properties of perineurium can be observed. From Figure 20, the percentage variation at different distances from the active site can be observed. 100% indicate the higher potential value found close to the active site, other values are the percentage variation compared to it. Observing the figure, it is possible to note that at 100µm of distance the electric potential decreases around 60% of the value close to the active site, for both the geometries. The points on the left of the plot are related to the fascicle where the active site is implanted in, the points on the right of the plot are related to another fascicle near to it. It is possible to observe that the trends related to both the simulations with different geometry are the same. Similar percentage variation are shown also

in the right part of the plot, related to the second fascicle. In both the plots the variation is lower than the 20% of the value near to the active site. From Figure 21 it is possible to observe that the trend about the electrical charge quantity necessary to activate 100% of fibers is similar using data from anatomical and simplified geometry. From both the plots it is possible to note that lower values of electric charge are required to activate fibers in the first fascicle.
These results are in accordance with the ones shown in the colormaps, in terms of fibers activation. From Figure 21a, b is evident that electrical charge values, related to the simplified geometry, are lower than the values related to the anatomical geometry. In particular electrical charge values found from the simplified geometry are around tens nC lower than the results related to the simulation of anatomical geometry.

3.4 CONCLUSIONS

Intraneural electrical stimulation is a high invasive technique that allows to restore tactile sensory feedback in the framework of upper limb prosthetics. Because of the high invasiveness, computational simulations can be used to design more efficient interfaces and to forecast their effects on the peripheral nerves and to provide guide lines to the surgeons on the modality of the implant related to the location of the electrodes in the nerve.
In this chapter, a computational hybrid FEM NEURON model was used to study the electric potential distribution in the human median nerve and the activation of axon fibers into it.
A 3D conductor model of an human median nerve and a 3D model of a ds-FILE electrode were developed to study the electric potential distribution resulting from an electrical intraneural current stimulation.
In addition, two other FEM computational simulations considering two different sensory fascicles and a motor fascicle were performed to investigate how an intraneural electrode fixed in a given location in the human median nerve can activate axon fibers of sensory or motor fascicles.
Subsequently, the results obtained using an anatomical nerve model and a simplified nerve model were compared to verify the possibility of considering the simplified model instead of the anatomical one in future computational simulation because it could represent a great advantage in terms of computational time for meshing and solution finding.
Results from the FEM model were elaborated in Matlab ®and imported in Neuron to study the axon fibers activation using three different types of stimulus waveforms. The results demonstrate that using a biphasic charge balanced stimulus waveform leads to an increase

of the current stimulation threshold and that the third waveform considered is the safer one because the threshold to activate a given percentage of fibers is lower than the threshold of the other stimuli. This research is useful to study in simulation the environment parameters for achieving axon fibers recruitment during an intraneural stimulation. As regards the simulations in sensory fascicle, active site in the inner part of the fascicle was considered and activation properties in ten different distances from the electrode for three type of waveform stimulus and at different values of current amplitude to obtain an activation percentage above 95% is studied. In the simulations in motor fascicles, a sensory fascicle close to the one analyzed in the first simulation and a motor fascicle were considered. The activation properties in ten different distances with respect to the inner part of each fascicle for three type of waveform as shown in Results and different values of current amplitude that let to obtain a percentage of activation above 95% are studied.

The obtained results demonstrated that related to the sensory fascicles studied, the current amplitude to activate axons increases according to the distance from the electrode and the third stimulus is the safest because compared with the other waveforms the same percentage of activation can be obtained using lower values of current amplitude. From the second simulation, it was observed that, if a stimulation of a sensory fascicle is performed using the current amplitude values considered in the results, the motor fascicle fiber was not activated, since the electric potential values are lower than the ones needed to activate the fiber. In fact, the needed value should be of one order of magnitude higher.

From the results related to the FEM-Neuron simulations using anatomical and simplified human median nerve models, it is possible to conclude as follows:

The first results, comparing the electric potential distributions from Comsol simulations, indicated that the values from the anatomical and simplified geometrical model are comparable less than a value of 0.0039 V. A similar percentage of activation is observed in anatomical and simplified model with a displacement of 20µA one to the other.

From the minimum electric charge necessary to activate the 100% of fibers at different distance from the active site it is possible to observe that also in this case the trends are similar related to the anatomical and simplified models.

4

A SIMULATION AND EXPERIMENTAL STUDY TO COMPARE ELECTRICAL NEURAL STIMULATION USING CUFF AND DS-FILE NEURAL ELECTRODES

4.1 INTRODUCTION

As discussed in the previous chapter, the study of electrical neural stimulation is of considerable interest because of the high invasiveness of the real solution. Besides the results discussed in the previous chapter another important aspect can be considered in the nerve-electrode interaction by computational models.

A comparative simulation study on the interaction between neural cuff electrode and ds-FILE intraneural electrode with human median nerve can be an useful approach to study the range of parameters to be used to stimulate the nerve and to evaluate the behaviour of the nerve fibers subjected to the electric current stimulus sent from the two different type of electrodes. At the same time, the evaluation of the simulation results related to activation properties and the comparison between experimental studies on human amputees can be an important approach to obtain more insight in the framework of electrical nerve stimulation to restore sensory feedback in the prosthetic research field. In the work of Oddo et al. 2016 [8] a section on the neurocomputational study with hybrid FEM-Neuron comparison of TIME and microneurographic electrodes is discussed. Anatomical data to obtain the FEM model were provided from [112] and the MRG model was used to describe the biophysics of axons in Neuron. TIME, microneedle electrodes and the anatomical median nerve were modelled by means of the FEM software Comsol Multiphysics and the electric potential into the nerve when a current stimulus was delivered by the two different electrodes was studied. That work includes also an experimental study on healthy and amputee subjects and how to provide the tactile texture discrimination is described.

PROGRESS BEYOND THE SOA In this chapter the novel contribution is related to: a comparative study of the activation fibers properties between electric neural stimulation using cuff and ds-FILE electrode using computational models; and a comparison between the simulation and experimental results on human amputee. It is noteworthy that there are not studies in literature that treat a comparison between the two electrodes considered from a simulation point of view, so to have more insight in this framework, estimating fibers activation properties in human median nerve subjected to electric current neural

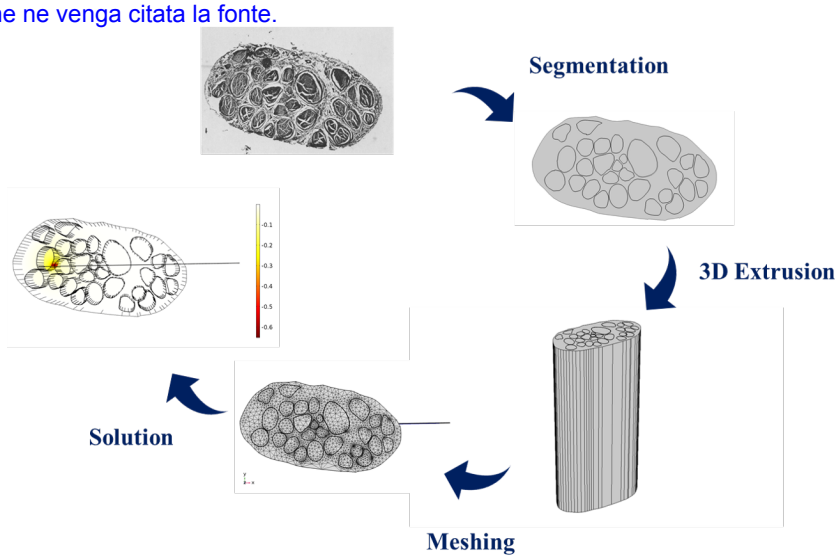

Figure 22: Schematic view of the procedure followed to obtain the FEM model solution, starting from the anatomical image of the median nerve.

stimulation can be useful. The comparison between the simulation results and experimental trials on human amputee is considered using two type of electrodes used in the human experimentation published in [7].

Chapter 4 is structured as follows: In Section 4.2 methods used to develop computational models of nerve-electrode interaction are discussed. Different steps to obtain a FEM model of nerve and electrodes and mathematical model of axon fibers are treated. In Section 4.3 results about the fibers activation for different values of electric charge using the ds-FILE and cuff electrodes using computational models are shown. The electric stimulus parameters are the same used in the experimental work [7], with the aims to compare experimental and simulation results. The results are commented and discussed in Section 4.4. Conclusions of this chapter are presented in Section 4.5.

4.2 METHODS

Two 3D finite element conductor models of the human median nerve have been developed according to the type of electrode considered following the same procedure shown in the previous chapter. Neural cuff electrode has a circular section. So the nerve subjected to the cuff implant could be modified in its section to a circular shape. In the model development, nerve section shape has been modified for the cuff electrode model simulation according to the shape and dimension of the cuff section. Inner fascicles of the nerve are considered in the original polygonal shape according to the anatomy of the nerve considered by the anatomical image [108]. Nerve section dimension

is different along the course of the nerve [109]. The two different electrode models in simulation environment are considered as implanted in different regions of the nerve according to the experimental study [7], so the nerve section considered in simulation with cuff has a value of surface area lower than the value considered in ds-FILE simulation. More details are discussed in Section 4.2.1.

The electric potential distributions into the nerve subjected to a current stimulus by the two electrode types are analyzed and processed in Matlab, different steps are in Section 4.2.3. These values are interpolated on different sections of the axon model in Neuron [106] to study the activation of nerve fibers. Simulations are performed on a computer with an Intel Core i7-8750H CPU at 2.20 GHz, 16 Gb RAM.

4.2.1 *FEM models of neural electrodes and human median nerve*

The human median nerve model can be obtained from its anatomical image, as treated in the previous chapter and summarized in Figure 22. According to the electrode type considered, two different nerve dimensions are modelled, depending on the different regions of implant of the different electrodes. Geometrical properties of the human median nerve are set according to the data reported in [109]. The nerve model subject to the cuff implant is reshaped according to the electrode section, from the ellipsis-type section of the anatomical image to a circle-type section according to the cuff section. The two median nerve 3D models are developed in Comsol Multiphysics ®v.5.3; both the models have a length of 15 mm, obtained by extruding the nerve section along the longitudinal axis. The 3D nerve model obtained by the extrusion assumes that the inner fascicles shape does not vary along the longitudinal direction, this assumption is considered according to [108] where it is found that the longest section with constant pattern was 15 mm.

Different tissue classes are assigned to each region of the nerve model according to the anatomy as treated in Section 3.2 and in Table 3.

A cylindrical region with saline solution properties and a diameter of 76 mm is considered to simulate the intraoperative environment. The equations considered are treated in Section 3.2.

Nerve dimension in the two models is different according to the electrode dimension and to the region of the nerve where the electrode is implanted in experimental studies.

Regarding the nerve model using cuff electrode, nerve section shape is modified to obtain a circular section, to simulate the implant of the electrode. It is assumed that the shape of the inner fascicles is not modified by the implant, but the fascicles are only translated to get in the circular section. This is an assumption similar to that reported in [113].

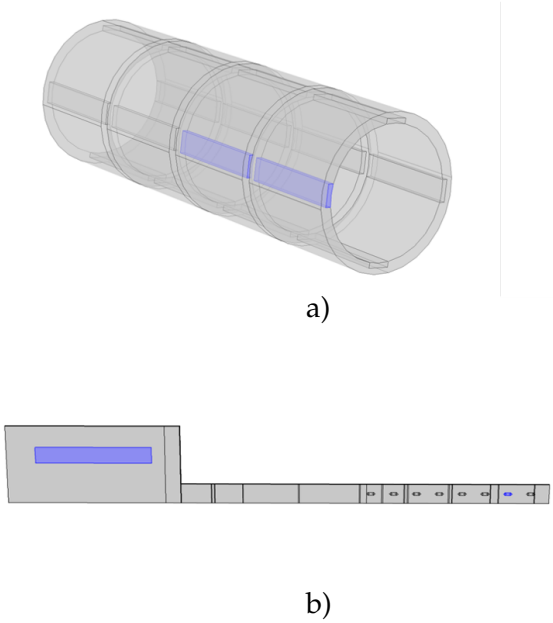

a)

b)

Figure 23: Electrodes CAD models. Cuff electrode model a) and ds-FILE electrode model b). Active sites used are highlighted in both the models.

4.2.2 *Electrode models*

The ds-FILE electrode model and the cuff electrode model (Figure 23) are developed in Comsol ®.

The ds-FILE electrode model is described in Section 3.2 and in [23], [107]. It is located at middle length of the nerve model and current intensity is set to an arbitrary value that will be subsequently modified in the Neuron axon model.

A similar procedure is followed to develop the cuff electrode. A sixteen active sites, cuff model is built. There are 14 active contacts and 2 ground distributed on 4 rings according to geometrical properties of the electrode model by Ardiem Medical. This model presents 16 platinum active sites with dimension 2.5 mm · 0.5 mm · 0.125 mm. As for the ds-FILE electrode, the material of the body is polymide. It has a conductivity of $6.7 \cdot 10^{-14}$ S/m, active sites have a conductivity of $8.9 \cdot 10^{6}$ S/m.

4.2.3 *Axon mathematical model*

The double cable MRG axon model, treated in Section 3.2 is used.

Data on electric potential distribution are exported from Comsol Multiphysics to Matlab and then processed and exported to Neuron to study the fibers activation. From the geometrical section of the median nerve, for each nerve fascicle considered, 100 fibers randomly located into the fascicles are modelled with different values of diame-

ters randomly extracted from two gaussian distributions [15]. Electric potential values are interpolated in Matlab on different regions of the nerve fibers and used in Neuron as extracellular potential. The stimulus waveform, defined as extracellular potential, is a biphasic charge balanced waveform, with pulse duration 80 µs, 50 Hz frequency and a current amplitude variation according to the type of electrode used, based on [7].

4.2.4 *Experimental data comparison*

In the study [7] on human amputee, electrical neural stimulation is used to restore sensory feedback in a human subject wearing a myoelectric hand prosthesis. Two biomechatronic hands were used: the IH2 Azzurra (Prensilia s.r.l) and the RoboLimb (TouchBionics s.r.l). They were equipped with force-sensing resistors (Interlink Electronics Inc.). Cuff and intraneural electrodes (ds-FILE) in median and ulnar nerve were implanted for 11 weeks to restore electrically tactile sensations. Sensory information, produced during the grasping and manipulation, came from force sensors located on the fingertips of the prosthetic hand. The signal is processed and sent to peripheral upper limb nerves, i.e. median and ulnar nerves. An intensity index is used to evaluate and quantify sensory information elicited by neural electrical stimulation. For each type of sensation an index range from 0 to 10 is considered, asking the patient what is the intensity of the felt sensation. The two different sensations elicited, as reported in Table 4 were obtained sending from ds-FILE or Cuff electrode active site a current signal with increasing intensity.

In this chapter, the same stimulation parameters used in human trials are considered in the simulation. To different current values of the stimuli, the number of activated fibers is associated. This number can be put in relation with the real tactile or movement sensation perceived by the subject.

4.3 RESULTS

A biphasic charge balanced waveform is used to stimulate nerve fibers alternatively using an intraneural ds-FILE electrode and a cuff electrode. All the stimulation parameters (pulse width, frequency, current intensity) are the same used in the experimental study on human amputee [7]. In particular, frequency and pulse width are fixed to 50 Hz and 80 µs respectively. Figure 24 shows the fiber Percentage of Activation as the electric charge quantity varies. Figure 24 a) concerns the percentage of activation of the nerve fascicle where the ds-FILE is inserted and of some fascicles close to it, while Figure 24 b) concerns the percentage of activation of some fascicles close to the active sites of the cuff electrode.

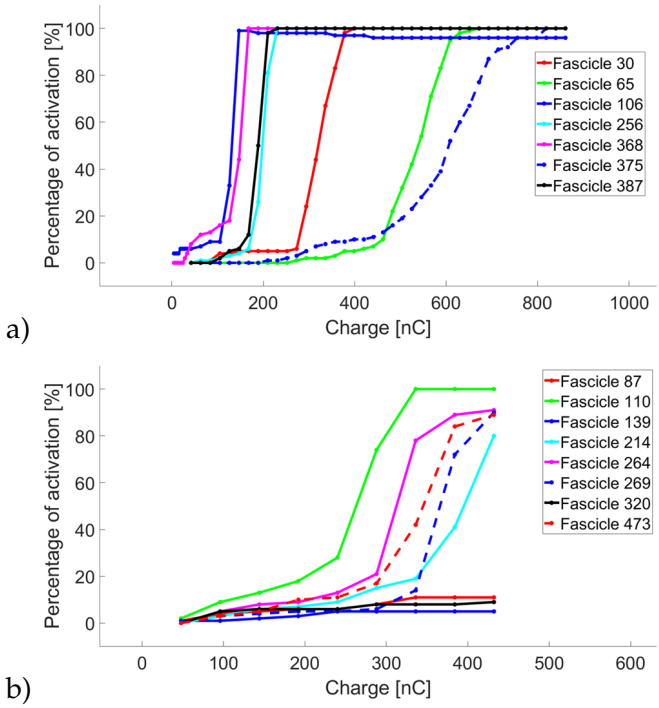

Figure 24: Percentage of Activation of fibers when the electric charge varies in case of the ds-FILE electrode Figure 24 a) and of the cuff electrode Figure 24 b).

A comparison was made between simulation and experimental results on human amputee. The considered electrical parameters are the same used in the mentioned experimental study when sensations are elicited in the amputee. In particular, when the ds-FILE electrode is used, frequency and pulse width are fixed to 50 Hz and 60 µs respectively. As for the cuff electrode, 50 Hz frequency and 200 µs pulse width are considered. The step size used are 50 µA and 100 µA for the simulations using ds-FILE and cuff electrode respectively.

In Figure 24 can be observed the Percentage of Activation when the electric charge varies related to the ds-FILE electrode Figure 24 a) and the cuff electrode Figure 24 b).

Figure 25, shows the percentage of activation when the electrical charge varies, for the ds-FILE (a) and cuff (b) electrodes. To obtain these plots, different sets of stimulation parameters are used, according to the ones employed in the experimental study on human amputee. In particular, these parameters are considered to compare sensations elicited in a human amputee with the percentage of activation of fibers. The electrical parameters are shown in Table 4.

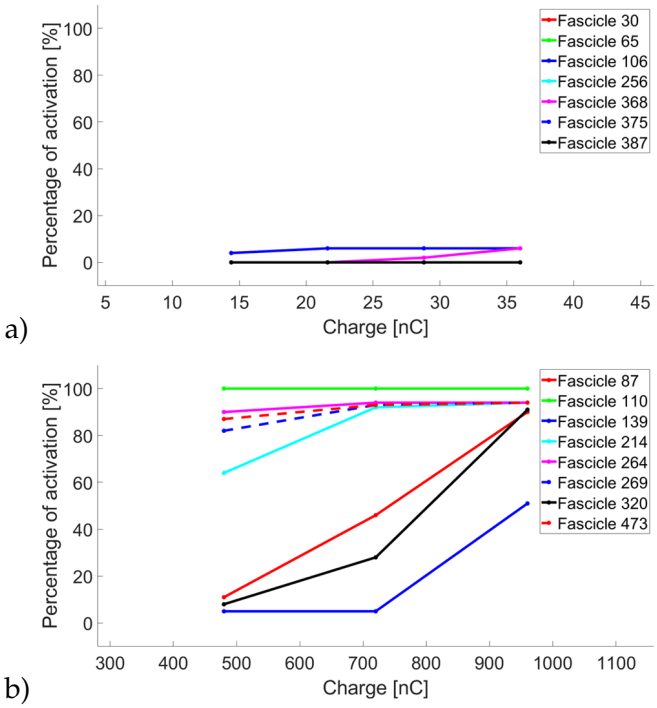

Figure 25: Percentage of Activation of fibers when the electric charge varies in case of the ds-FILE electrode Figure 25 a) and of the cuff electrode Figure 25 b), using the same parameters shown in Table 4

4.4 DISCUSSION

Computer simulation using hybrid FEM-Neuron model is an useful approach for studying the electrical response of neural tissues subjected to electric current stimulation. Knowing the neural fascicle activation modalities allows to evaluate the optimal electrical parameter to be used, the location of the electrode and the active sites that have to be used. Therefore, the percentage of activation in some fascicles has been studied by considering 100 fibers randomly located in each fascicle. Each fiber has a diameter randomly extracted from a bigaussian distribution.

In Figure 24 a), the typical trend of the fiber activation curve when the electrical charge increases, for the different nerve fascicles, during the stimulation with the ds-FILE electrode, is shown. It is possible to note that the first fascicles with activated fibers are those labeled 106 and 368, i.e., the fascicle inside which there is the active site and the one closer to it. The number of fibers in the other fascicles are gradually activated as the electric charge increases.

In Figure 24 b), the typical trend of the fiber activation curve when the electrical charge increases, for the cuff electrode, is shown. Also in this case, fibers close to the boundary of the nerve are activated first, (active sites of the cuff electrode are located around the nerve).

Table 4: Set of stimulation parameters used in the experimental trials. To each current intensity value a different intensity sensation elicited in the amputee corresponds

Electrode model	Frequency (Hz)	Pulse Width (μs)	Electric current (μA)	Sensation elicited	Sensation intensity (a.u.)
ds-FILE	50	60	40	middle finger metacarpophalangeal flexion	0
			60		3
			80		7
			100		7
Cuff	50	200	400	middle finger flexion	2
			600		3
			800		6

Hence, fibers close to the boundary are activated at lower values of electrical charge than the fibers in the inner of the nerve.

If we compare the results obtained by using the two different electrodes, it is possible to note that the cuff electrode needs higher values of electrical charge to stimulate fibers starting from around 50 nC. Otherwise, the electrical charge needed by the ds-FILE electrode starts from tens of nC, and the seven fascicles considered have all the fibers activated when the electrical charge reaches about 600 nC. In the simulation using the cuff electrode, the first fibers are activated at around 50 nC in the fascicles close to the active site of the electrode. Other fibers are activated up to 400 nC, but, as shown in the Figure 24, the fibers further from the active sites are activated at higher values. The value of 400 nC is not enough to activate them.

From Figure 25 a) and Table 4, it is possible to observe that, as the electric charge increases, more fibers are activated in some fascicles. Note that not all the fascicles considered have activated fibers, because the range of values are lower than for the previous sets of parameters. To different values of electrical charge an increasing percentage of activation corresponds; this is expressed, in the experimental situation, by an increasing intensity of the sensation perceived by the amputee.

Similar considerations can be done in relation to the cuff results. In Figure 25 b), showing the plot relating to the cuff, it can be seen that fibers activation increases according to the electrical charge and in Table 4 it is evident that the intensity of sensation elicited in the amputee increases as the electric current increases.

A higher number of fibers activated in simulation corresponds to a more intense sensation felt by the amputee in the experimental trial. The computational simulations treated in this sections could be used also to study the selectivity of both the electrodes. A simulation study considering all the fascicles of the median nerve and in each fascicles a different number of axons has to be considered. In each simulations, one by one active site of the electrode has to be used to send the current stimulus. Studying the number of fascicles recruited without recruit the other can be estimated the selectivity of the active sites.

4.5 CONCLUSIONS

In this chapter the neural fiber activation by electric current stimulation using ds-FILE and cuff electrodes has been analyzed by means of the FEM-Neuron computational approach.

In the first part of the study, according to the two different electrode models, two different FEM simulations using Comsol Multiphysics were performed. Differences between the two electrode configurations in terms of fibers activation are shown using the same electrical parameters except for current intensity that is specifically related to intraneural or extraneural electrodes.

In the second part of the study, stimulation parameters used in the experimental study on a human amputee are used and fiber activation results are compared with sensations elicited in the experimental study.

As regards the first part, a typical trend of the fiber activation is observed. More fibers are activated when the electric charge increases, using both the electrode types. The number of fascicles activated increases according to the position with respect to the active sites, starting from the closer one.

The second part of the chapter highlights that to the increase of the sensation intensity elicited in the amputee subject, an increasing value of fibers activated in different fascicles corresponds in the simulations results.

5

SAFETY AND EFFICACY OF TFUS STUDIED IN A SIMULATION FRAMEWORK

5.1 INTRODUCTION

Brain stimulation methods can be used to modulate cortical areas, for functional investigation of the brain and neurotherapeutics. The most used non-invasive techniques, such as Transcranial Magnetic Stimulation (TMS) and Transcranial Direct Current Stimulation (TDCS), can modulate the function of cortical areas without the need of a surgical intervention [114–116]. These techniques permit the stimulation of large cortical areas, on the order of centimeters, whereas the possibility of reaching deep cortical regions is very limited [117]. Therefore, as an alternative, other non-invasive techniques are being investigated to overcome this shortcoming.

The tFUS is a non-invasive method, for the stimulation of both the Central and the Peripheral Nervous System, that has a better spatial resolution and in-depth penetration with respect to other transcranial stimulation techniques, such as TDCS and TMS.

In fact, tFUS is a low energy technique delivering mechanical energy at high spatial resolution [14] that has been shown to be capable of modulating neural activity in mice [118, 119], rabbits [120] and monkeys [121]. Recent studies demonstrate that tFUS is also a safe and effective technique able to modulate human cortical activity [13, 122]. Ultrasonic neuromodulation on Central Nervous System can be applied on M1 cortex, Thalamus, V1 cortex, caudate region and posterior frontal cortex in humans [13, 122–125].

As treated in Chapter 1, recently, the use of tFUS as non-invasive brain stimulation technique was proven to be able to elicit tactile sensations when applied on S1 and S2 cortex [14, 124, 126–129]. It paves the way to its application in neuroprosthetics for restoring sensory feedback in amputee subjects. In particular, this technique can be an important alternative (as tFUS applied to CNS or as FUS applied to PNS) to the direct electric current stimulation treated in the previous chapters to restore sensory feedback in upper limb prosthesis users in a non-invasive way.

Nevertheless, even if tFUS is a non-invasive method, attention needs to be paid to the power intensity applied on the target area. For instance, the temperature increases due to the acoustic intensity conveyed to the scalp could damage tissues if not kept below a safety threshold. Therefore, the signal intensity and the stimulation duration cannot overcome safety limits. It is evident that a preliminary

study of tFUS outcome in simulation environment is extremely important. Computational models have been used to estimate power intensity and pressure profiles in biological tissues, considering anatomical variations between individuals [130, 131].

No studies have been performed to understand if the waveform modulation allows keeping the safety limits and the stimulation efficacy by reducing the stimulation intensity. Studies performed on other non-invasive stimulation techniques (such as transcutaneous electrical nerve stimulation, TENS), where the variation of the stimulation intensity (in terms of duration of the stimulation) can elicit different sensations in different hand areas [132], suggest that also with tFUS it is possible to vary the stimulation duration for eliciting different sensations. The main advantage of using tFUS with respect to other non-invasive stimulation approaches [133] relies in the possibility of achieving high selectivity stimulation and discrimination capabilities similar to invasive interfaces.

PROGRESS BEYOND THE SOA The contribution of Chapter 5 is to investigate, by means of a computational model, if pulsed stimulation with a modulated waveform may be effective in terms of provided pressure and safe in terms of intensity. In other words, the scope is to ascertain whether it is possible to modulate the stimulation wave so that it has the same effectiveness, without affecting pressure, but with lower intensity and increased duration, with respect to stimulation waves typically adopted in literature.

Chapter 5 is structured as follows: in Section 5.2 methods used to develop computational simulation are trated. The approach using a specific Matlab toolbox for the time-domain simulation of acoustic wave fields is described, considering different tissues physical properties and modeling in a simplified way the surface of an ultrasound commercial transducer and human head in 2D geometry. In Section 5.3 results about the pressure and power intensity field in free water and through the skull are presented for different values of Duty Cycle of the stimulus. These results are commented and discuessed in Section 5.4. Conclusions of this chapter are presented in Section 5.5.

	c_s [m/s^2]	ρ [kg/m^3]	α_0 [dB/MHz · cm]
Water [134]	1481	998	0.002
Skull [134]	2820	1732	7.75
Brain [135]	1500	1000	0.8

Table 5: Media properties. c_s: sound velocity in medium; ρ: density of the medium; α_0: medium constant to evaluate the absorption coefficient

In this study, a 2D simplified human head model composed of a skull layer and brain tissue was considered. The ultrasound coupling medium was also modelled and the physical properties of each media were summarized in Table 5.
The propagation of the focused ultrasound was simulated in the 2D simplified human head model in order to investigate the maximum pressure amplitude, the mean intensity and the focus profile for different Duty Cycle (DC). The simulations were performed using a k-space pseudospectral method-based solver, i.e. k-Wave [19].
Simulations were performed on a computer with an Intel Core i7-8750H CPU at 2.20 GHz, 16GB RAM.

In Figure 26 the model is described. The transducer was modeled as an arc circle, 63.2 cm radius of curvature, based on a commercial ultrasound transducer, i.e. Sonic Concepts H-115 model. Two concentric circles modeled the brain and skull regions. Properties of the brain were assigned to the most inner region; whereas properties of skull were assigned to the ring area obtained from the outer circle (diameter of 77.5 mm) and the inner one (diameter of 72 mm). A 4 cm distance was considered between the arc circle and the outer circle of the skull layer. The properties of water were given to this domain. These properties are taken from [3].

Water, skull and brain were assumed to have different sound speed, density and attenuation coefficient.

A 20 cm $\times$ 20 cm simulation grid was considered to observe the focus profile in terms of maximum pressure amplitude (Pa) and average acoustic intensity (W/m^2).

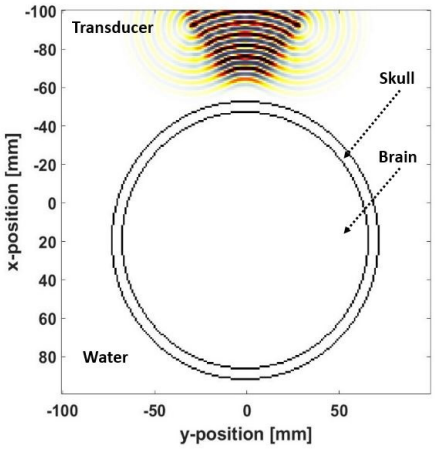

Figure 26: The domain is composed of the transducer surface, the skull layer, the brain region and the water, which is the surrounding medium.

2D maps of coupling water, skull layer and brain were extracted for different values of the pulse duty cycle. Several simulations were

performed varying the DC of the stimulus: it was varied from 100% to 40% with a step of 10%, tightening the step in the range from 50% to 40%.
To restrict the computation time, the total duration of the simulation was limited to 500 µs (DC of 100%) and the minimum duration of the pulse stimulus was fixed at 200 µs (DC of 40%), which was above the necessary duration t_{ss} (190 µs) to reach a steady-state. This value was obtained as follows

$$t_{ss} = \frac{\sqrt{{s_x}^2 + {s_y}^2}}{v_s} \tag{25}$$

where s_x and s_y are the grid lengths in the x and y direction, respectively, and v_s is the minimum sound velocity in the medium evaluated between the considered media. The pulse stimulus was a sinusoidal waveform settled at a frequency of 250 kHz, which was the value used in tFUS experiments to somatosensory cortex stimulation on humans.

The amplitude of the sinusoidal waveform was fixed for all the simulations at 100 kPa. This value was determined during the free water simulation lasting 500 µs, in order to obtain a maximum average intensity under the safety threshold (3 W/cm^2 according to the IEC standard 60601-2-5 for physiotherapy US equipment).

For each DC value, two simulations were performed: one in free water and one with the coupling medium (water), skull and brain layers. Hence, it was possible to compare the behaviour of the beams in the two different domains in terms of maximum pressure and average acoustic intensity. The data extracted from the simulation were used to analyse the evolution of the maximum pressure and the average intensity in the focus modulating the DC of the pulse stimulus. Moreover, Full Width at Half Maximum (FWHM) of the average intensity profile on the focal plane was evaluated in order to observe the focal width, when DC was varied.

5.3 RESULTS

In the following section the behaviour of the maximum pressure and average intensity in water and in layered media obtained in simulation are described. Simulations were performed at eight different values of DC signal: 100%, 90%, 80%, 70%, 60%, 50%, 45% and 40%. A 100% DC and a 40% DC correspond to a stimulus duration of 500 µs and 200 µs, respectively.
The maximum pressure and the average acoustic intensity profile for a 100% DC in free water simulation are shown in Figure 27 (**a**) and Figure 28 (**b**) respectively. This simulation was performed varying the amplitude of the stimulus until the average acoustic intensity in the focus was about 3 W/cm^2. The obtained stimulus amplitude value was adopted for the remaining simulations.

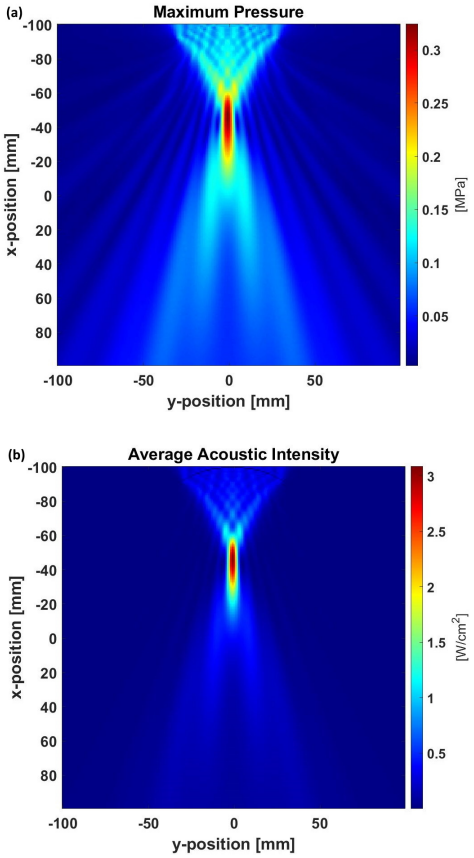

Figure 27: 2D grid color map of maximum pressure (**a**) and average acoustic intensity (**b**) for a 100% DC stimulus obtained from the simulation in free water.

In Figure 28 the maximum values of pressure and average intensity are reported for each stimulus DC for the free water and layered medium simulations.
FWHM of average intensity profile along y-axis was studied for the different simulations to observe the focal width at different value of the signal DC. The data extracted for each DC during the simulation in water and with the layered medium, were fitted and shown in Figure 29, where the fitting using a Gaussian function of the average intensities can be observed.

5.4 DISCUSSION

Maximum pressure amplitude and average intensity (Figure 27) were studied in free water at a 100% DC signal, to evaluate the maximum of average intensity in the focus according to the safety threshold. The corresponding stimulus amplitude was adopted in all the subsequent simulations. Comparing the maximum pressure amplitude color plot related to each stimulus DC for water and layered medium, it is pos-

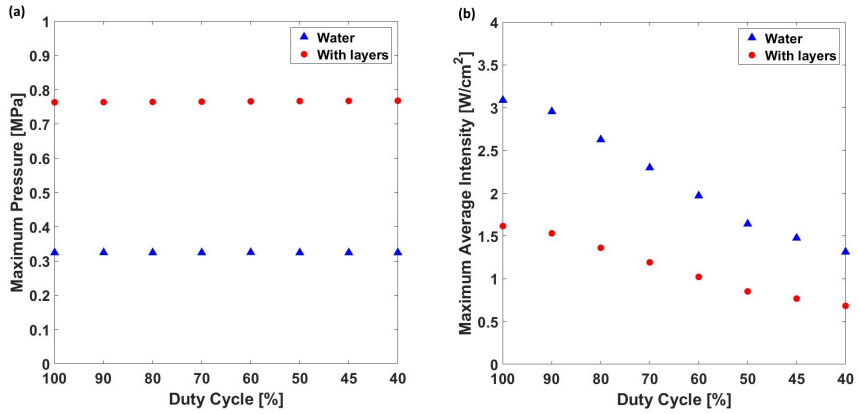

Figure 28: Pressure and Maximum Average Intensity variation at different DC. (**a**) Maximum Pressure *vs* Duty Cycle in water and layered media; (**b**) Maximum Average Intensity *vs* Duty Cycle in water and layered media

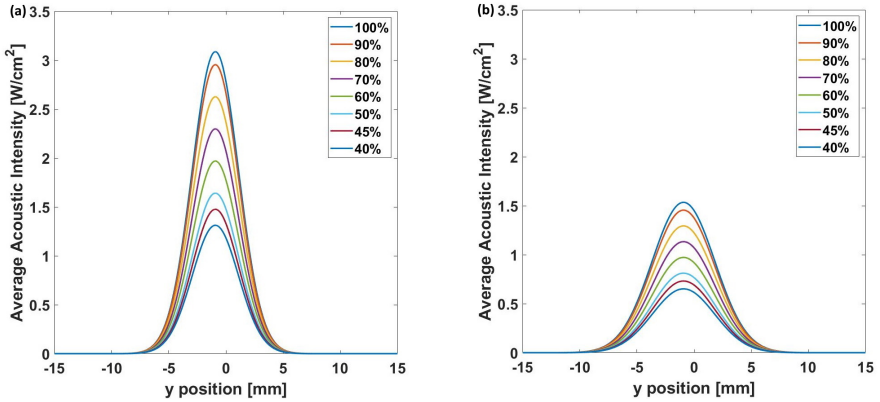

Figure 29: Average Intensity profile on the focal plane *vs* y position in water and layered media for different values of DC. (**a**) Average Intensity *vs* y position in free water; (**b**) Average Intensity *vs* y position in layered medium

sible to observe that the stimulation was effective since the value of maximum pressure was comparable with that of the steady-state.

Literature studies on the effects of the tFUS stimulus on the generation of action potentials in neuronal cells, hypothesized that the amplitude of an external pressure, i.e. the pressure stimulus coming from the transducer, and the stimulus duration can affect the generation of the action potentials [136]. This suggests that the pressure term can be seen as an index of stimulation efficacy.

Looking at the results shown in Figure 28 (**a**), it was evident that a decrease of the pulse stimulus DC did not affect the values of the maximum pressure, meaning that the stimulation efficacy remained unchanged. Therefore, to deliver a signal that has a low value of DC, can be more safe and equally effective compared to stimulus signals that have higher DC values, Figure 28 (**b**). These results would lead

to the possibility of increasing the stimulus duration, maintaining the safety and the efficacy of the stimulations.

The evaluation of the focal width could have been useful to verify that the stimulation occurred in a specific region of the considered tissue. From Figure 29, it is evident that the FWHM was almost the same for different values of signal DC. Therefore, to deliver a signal at low DC values do not affect the spatial resolution or selectivity of the stimulation.

5.5 CONCLUSION

In this chapter, the study on a computational model for analyzing the maximum pressure and average acoustic intensity occurring during tFUS stimulation is described. Two simulations on focused ultrasound in water and through a skull layer were performed to investigate the effect of focused ultrasound stimulation on biological tissues. In the free water simulation the entire domain was homogeneously modeled as water. For the layered simulation the medium was a simplified head model. They were developed to compare pressure and intensity at the focus from both the simulations. A 2D simplified human head model was considered to guarantee low computational complexity and estimated simulation time.

Although in a preliminary computational framework, the obtained results demonstrated i) that a geometrical simplified human head model could be a useful tool for estimating the main values related to efficacy and safety of tFUS; ii) the possibility to investigate, from a theoretical point of view, how to modulate the stimulation waveform, with the aim to keep constant the efficacy and the safety of tFUS.

The obtained results could be confirmed by experimental validation starting from tissue-mimicking phantom materials before the tests on human subjects.

6 CONCLUSION

In this thesis, two different techniques used to restore sensory feedback in amputees are studied by means of computational models focusing on the multiscale approach.
Properties of neural cells in main animal models and in human are discussed considering the ion channel found in different species. The main mathematical models used to describe neural cells and axons are discussed. From the different mathematical models found in literature the MRG axon model is the more suitable to be used in multiscale model for peripheral neural stimulation. The MRG model is a double cable axon model taking into account nodal and internodal sections, myelin sheath and temperature feedback. Moreover, the multiscale approach is discussed to couple the FEM model approach with the mathematical model of axon. So the first chapter of this thesis can be a useful guideline to develope multiscale model for electrical neural stimulation of peripheral fibers.

Subsequently, the multiscale FEM-Neuron approach is used to study the electric neural stimulation of human median nerve. From the analysis of different waveform stimuli the biphasic charge unbalanced stimulus is the better choice in terms of efficacy and safety. This observation can be considered also from the discussion of the percentage of activation necessary to activate fibers from 95% to 100%. We observed that using the biphasic unbalanced stimulus waveform the same percentage of activation is obtained using lower values of current amplitude. To observe how far the intraneural electrode can activate fibers, the percentage of activation is studied at different distances from the active site in two sensory fascicles and in one motor fascicles. From the results we concluded that fibers in motor fascicle are not activated applying the range of current used and that the current amplitude to activate axons increases according to the distance from the electrode in the considered fascicle.

As far as it concerns the simulations, a possibility to reduce computational time is discussed. The geometrical complexity of the human median nerve model is modified simplifying the section shape of inner fascicles with an approximation to elliptical shape. From the results it is observed that similar electric potential distribution are found in the models. The results about the minimum electric charge necessary to activate 100% of fibers at differen distances from the electrode, permit to conclude that the values found using the simplified geometry of the nerve are lower of tens of nC than the results found using the anatomical geometry.

Another study is considered to compare the behaviour of two different electrode models in its interaction with the nerve and a comparison between fibers activation using the same electrodes and experimental data on human amputee.

From the comparison obtained from the simulations related to the fiber activation when the electrical charge varies using ds-FILE and cuff electrodes a typical trend of the fiber activation is observed. When the electrical charge increases, more fibers are activated in both the simulations using ds-FILE and cuff electrode. The number of activated fibers in the fascicles increases according to the distance from the active sites.

From the simulations performed using the same electrical stimulus parameters applied in the experimental trial on humans, it is observed that to the increase of the sensation intensity elicited in the amputee subject, an increasing value of fibers activated in different fascicles corresponds in the simulation results.

Another technique to restore sensory feedback in human amputee is studied using computational simulations. The tFUS is an efficient low invasive technique but if more high power is used the possibility to damage tissues can be verified. So the simulation study is an important step before the in vivo test. From this study it is possible to investigate the modulation of stimulation waveform keeping the efficacy and safety of the stimulation.

Future works will be addressed to study different locations of the ds-FILE electrode into the nerve and different configurations of active sites for ds-FILE and cuff electrodes. These activities could be useful to evaluate the selectivity of the electrodes.

PUBLICATIONS

- Mattia STEFANO, Alessia Scarpelli, Francesca Cordella, Loredana Zollo, **A simulation study in safety and efficacy of tFUS**, VII Congress of the National Group of Bioengineering (GNB), 2020;
- Mattia STEFANO, Francesca Cordella, Loredana Zollo, **The intraneural electrical stimulation of human median nerve: a simulation study**, 2020 IEEE RO-MAN Conference;
- Mattia STEFANO, Francesca Cordella, Eugenio Guglielmelli, Loredana Zollo, **Intraneural electrical stimulation of median nerve: a simulation study on sensory and motor fascicles**, Journal of Biological Regulators and Homeostatic Agents, 2020;
- Mattia STEFANO, Francesca Cordella, Alessandro Loppini, Simonetta Filippi, Loredana Zollo, **A multiscale approach to axon and nerve stimulation modeling: A review**, IEEE Transactions on Neural Systems and Rehabilitation Engineering, 2021;
- Mattia STEFANO, Francesca Cordella, Salvatore Maria Li Gioi, Loredana Zollo, **Electrical Stimulation of the Human Median Nerve: A Comparison between Anatomical and Simplified Simulation Models**, IEEE Conferencee of Neural Engineering, 2021.

BIBLIOGRAPHY

[1] Daniel R Merrill, Marom Bikson, and John GR Jefferys. "Electrical stimulation of excitable tissue: design of efficacious and safe protocols." In: *Journal of neuroscience methods* 141.2 (2005), pp. 171–198.

[2] Deep-Brain Stimulation for Parkinson's Disease Study Group. "Deep-brain stimulation of the subthalamic nucleus or the pars interna of the globus pallidus in Parkinson's disease." In: *New England Journal of Medicine* 345.13 (2001), pp. 956–963.

[3] Enver Salkim, Arsam Shiraz, and Andreas Demosthenous. "Impact of neuroanatomical variations and electrode orientation on stimulus current in a device for migraine: a computational study." In: *Journal of Neural Engineering* 17.1 (2020), p. 016006.

[4] Mark S Humayun, James D Weiland, Gildo Y Fujii, Robert Greenberg, Richard Williamson, Jim Little, Brian Mech, Valerie Cimmarusti, Gretchen Van Boemel, Gislin Dagnelie, et al. "Visual perception in a blind subject with a chronic microelectronic retinal prosthesis." In: *Vision research* 43.24 (2003), pp. 2573–2581.

[5] Claudia A Angeli, V Reggie Edgerton, Yury P Gerasimenko, and Susan J Harkema. "Altering spinal cord excitability enables voluntary movements after chronic complete paralysis in humans." In: *Brain* 137.5 (2014), pp. 1394–1409.

[6] Francesca Cordella et al. "Literature review on needs of upper limb prosthesis users." In: *Frontiers in neuroscience* 10 (2016), p. 209.

[7] Loredana Zollo et al. "Restoring tactile sensations via neural interfaces for real-time force-and-slippage closed-loop control of bionic hands." In: *Science robotics* 4.27 (2019), eaau9924.

[8] Calogero Maria Oddo, Stanisa Raspopovic, Fiorenzo Artoni, Alberto Mazzoni, Giacomo Spigler, Francesco Petrini, Federica Giambattistelli, Fabrizio Vecchio, Francesca Miraglia, Loredana Zollo, et al. "Intraneural stimulation elicits discrimination of textural features by artificial fingertip in intact and amputee humans." In: *elife* 5 (2016), e09148.

[9] Alberto Mazzoni, Calogero M Oddo, Giacomo Valle, Domenico Camboni, Ivo Strauss, Massimo Barbaro, Gianluca Barabino, Roberto Puddu, Caterina Carboni, Lorenzo Bisoni, et al. "Morphological neural computation restores discrimination of naturalistic textures in trans-radial amputees." In: *Scientific reports* 10.1 (2020), pp. 1–14.

[10] Stanisa Raspopovic et al. "Restoring natural sensory feedback in real-time bidirectional hand prostheses." In: *Science translational medicine* 6.222 (2014), 222ra19–222ra19.

[11] Paolo M Rossini et al. "Double nerve intraneural interface implant on a human amputee for robotic hand control." In: *Clinical neurophysiology* 121.5 (2010), pp. 777–783.

[12] Daniel W Tan, Matthew A Schiefer, Michael W Keith, James Robert Anderson, Joyce Tyler, and Dustin J Tyler. "A neural interface provides long-term stable natural touch perception." In: *Science translational medicine* 6.257 (2014), 257ra138–257ra138.

[13] Wynn Legon, Priya Bansal, Roman Tyshynsky, Leo Ai, and Jerel K Mueller. "Transcranial focused ultrasound neuromodulation of the human primary motor cortex." In: *Scientific reports* 8.1 (2018), pp. 1–14.

[14] Wonhye Lee, Yong An Chung, Yujin Jung, In-Uk Song, and Seung-Schik Yoo. "Simultaneous acoustic stimulation of human primary and secondary somatosensory cortices using transcranial focused ultrasound." In: *BMC neuroscience* 17.1 (2016), pp. 1–11.

[15] Stanisa Raspopovic et al. "Framework for the development of neuroprostheses: from basic understanding by sciatic and median nerves models to bionic legs and hands." In: *Proceedings of the IEEE* 105 (2016).

[16] Enver Salkim, Arsam Shiraz, and Andreas Demosthenous. "Effect of model complexity on fiber activation estimates in a wearable neuromodulator for migraine." In: *2017 IEEE Biomedical Circuits and Systems Conference (BioCAS)*. IEEE. 2017, pp. 1–4.

[17] Marek Zelechowski, Giacomo Valle, and Stanisa Raspopovic. "A computational model to design neural interfaces for lower-limb sensory neuroprostheses." In: *Journal of neuroengineering and rehabilitation* 17.1 (2020), pp. 1–13.

[18] Arsam N Shiraz et al. "Minimizing stimulus current in a wearable pudendal nerve stimulator using computational models." In: *IEEE TNSRE* 24.4 (2016), pp. 506–515.

[19] Bradley E Treeby, Jiri Jaros, Alistair P Rendell, and BT Cox. "Modeling nonlinear ultrasound propagation in heterogeneous media with power law absorption using ak-space pseudospectral method." In: *The Journal of the Acoustical Society of America* 131.6 (2012), pp. 4324–4336.

[20] M. Stefano et al. "A multiscale approach to axon and nerve stimulation modeling: A review." In: *IEEE TNSRE* (2021). DOI: 10.1109/TNSRE.2021.3054551.

[21] Mattia Stefano et al. "The intraneural electrical stimulation of human median nerve: a simulation study." In: *2020 IEEE RO-MAN Conference*.

[22] M Stefano et al. "Intraneural electrical stimulation of median nerve: a simulation study on sensory and motor fascicles." In: *J. of Biol. Reg. and Hom. Ag.* (2020).

[23] Mattia Stefano, Francesca Cordella, Salvatore M. Li Gioi, and Loredana Zollo. "Electrical Stimulation of the Human Median Nerve: A Comparison between Anatomical and Simplified Simulation Models." In: *IEEE Conference of Neural Engineering* (2021).

[24] Mattia Stefano, Alessia Scarpelli, Francesca Cordella, and Loredana Zollo. "A simulation study in safety and efficacy of tFUS." In: *VII Congress of the National Group of Bioengineering (GNB)* (2020).

[25] Katharine H Polasek, Harry A Hoyen, Michael W Keith, Robert F Kirsch, and Dustin J Tyler. "Stimulation stability and selectivity of chronically implanted multicontact nerve cuff electrodes in the human upper extremity." In: *IEEE transactions on neural systems and rehabilitation engineering* 17.5 (2009), pp. 428–437.

[26] LE Fisher, DJ Tyler, JS Anderson, and RJ Triolo. "Chronic stability and selectivity of four-contact spiral nerve-cuff electrodes in stimulating the human femoral nerve." In: *Journal of neural engineering* 6.4 (2009), p. 046010.

[27] Stanisa Raspopovic, Marco Capogrosso, and Silvestro Micera. "A computational model for the stimulation of rat sciatic nerve using a transverse intrafascicular multichannel electrode." In: *IEEE Transactions on Neural Systems and Rehabilitation Engineering* 19.4 (2011), pp. 333–344.

[28] David Moher, Alessandro Liberati, Jennifer Tetzlaff, Douglas G Altman, et al. "Preferred reporting items for systematic reviews and meta-analyses: the PRISMA statement." In: *Int J Surg* 8.5 (2010), pp. 336–341.

[29] H Yu Frank and William A Catterall. "Overview of the voltage-gated sodium channel family." In: *Genome biology* 4.3 (2003), pp. 1–7.

[30] Ruxandra Barzan, Friederike Pfeiffer, and Maria Kukley. "N- and L-type voltage-gated calcium channels mediate fast calcium transients in axonal shafts of mouse peripheral nerve." In: *Frontiers in cellular neuroscience* 10 (2016), p. 135.

[31] SY Chiu, JM Ritchie, RB Rogart, and D Stagg. "A quantitative description of membrane currents in rabbit myelinated nerve." In: *The Journal of physiology* 292.1 (1979), pp. 149–166.

[32] Johannes Fleckenstein, Ruth Sittl, Beate Averbeck, Philip M Lang, Dominik Irnich, and Richard W Carr. "Activation of axonal Kv7 channels in human peripheral nerve by flupirtine but not placebo-therapeutic potential for peripheral neuropathies: results of a randomised controlled trial." In: *Journal of translational medicine* 11.1 (2013), pp. 1–13.

[33] T Brismar. "Potential clamp analysis of membrane currents in rat myelinated nerve fibres." In: *The Journal of physiology* 298.1 (1980), pp. 171–184.

[34] Andreas Scholz, Gordon Reid, Werner Vogel, and Hugh Bostock. "Ion channels in human axons." In: *Journal of neurophysiology* 70.3 (1993), pp. 1274–1279.

[35] Gordon Reid, Andreas Scholz, Hugh Bostock, and Werner Vogel. "Human axons contain at least five types of voltage-dependent potassium channel." In: *The Journal of physiology* 518.3 (1999), pp. 681–696.

[36] MN Rasband and James Trimmer. "Ion channel localization in axons." In: *Encyclopedia of neuroscience*. Elsevier Ltd, 2010, pp. 229–235.

[37] B Rudy, J Maffie, Y Amarillo, B Clark, EM Goldberg, HY Jeong, I Kruglikov, E Kwon, M Nadal, and E Zagha. "Voltage gated potassium channels: Structure and function of Kv1 to Kv9 subfamilies." In: *Encyclopedia of Neuroscience* 10 (2009), pp. 397–425.

[38] Manuel de Lera Ruiz and Richard L Kraus. "Voltage-gated sodium channels: structure, function, pharmacology, and clinical indications." In: *Journal of medicinal chemistry* 58.18 (2015), pp. 7093–7118.

[39] Alan L Goldin, Robert L Barchi, John H Caldwell, Franz Hofmann, James R Howe, John C Hunter, Roland G Kallen, Gail Mandel, Miriam H Meisler, Yoheved Berwald Netter, et al. "Nomenclature of voltage-gated sodium channels." In: *Neuron* 28.2 (2000), pp. 365–368.

[40] Tianbo Li and Jun Chen. "Voltage-Gated Sodium Channels in Drug Discovery." In: *Ion Channels in Health and Sickness*. IntechOpen, 2018.

[41] James L Salzer, Peter J Brophy, and Elior Peles. "Molecular domains of myelinated axons in the peripheral nervous system." In: *Glia* 56.14 (2008), pp. 1532–1540.

[42] T.P. Snutch. "Voltage-Gated Calcium Channels." In: *Encyclopedia of Neuroscience*. Ed. by Larry R. Squire. Oxford: Academic Press, 2009, pp. 427–441. ISBN: 978-0-08-045046-9. DOI: https://doi.org/10.1016/B978-008045046-9.01370-X. URL:

https://www.sciencedirect.com/science/article/pii/B978008045046901370X.

[43] Bruce Alberts, Alexander Johnson, Julian Lewis, Martin Raff, Keith Roberts, and Peter Walter. "Ion channels and the electrical properties of membranes." In: *Molecular Biology of the Cell. 4th edition*. Garland Science, 2002.

[44] Maarten HP Kole and Greg J Stuart. "Signal processing in the axon initial segment." In: *Neuron* 73.2 (2012), pp. 235–247.

[45] Amandine Duflocq, Barbara Le Bras, Erika Bullier, François Couraud, and Marc Davenne. "Nav1. 1 is predominantly expressed in nodes of Ranvier and axon initial segments." In: *Molecular and Cellular Neuroscience* 39.2 (2008), pp. 180–192.

[46] Audra Van Wart, James S Trimmer, and Gary Matthews. "Polarized distribution of ion channels within microdomains of the axon initial segment." In: *Journal of Comparative Neurology* 500.2 (2007), pp. 339–352.

[47] Ikuo Ogiwara, Hiroyuki Miyamoto, Noriyuki Morita, Nafiseh Atapour, Emi Mazaki, Ikuyo Inoue, Tamaki Takeuchi, Shigeyoshi Itohara, Yuchio Yanagawa, Kunihiko Obata, et al. "Nav1. 1 localizes to axons of parvalbumin-positive inhibitory interneurons: a circuit basis for epileptic seizures in mice carrying an Scn1a gene mutation." In: *Journal of Neuroscience* 27.22 (2007), pp. 5903–5914.

[48] Tatiana Boiko, Matthew N Rasband, S Rock Levinson, John H Caldwell, Gail Mandel, James S Trimmer, and Gary Matthews. "Compact myelin dictates the differential targeting of two sodium channel isoforms in the same axon." In: *Neuron* 30.1 (2001), pp. 91–104.

[49] Tatiana Boiko, Audra Van Wart, John H Caldwell, S Rock Levinson, James S Trimmer, and Gary Matthews. "Functional specialization of the axon initial segment by isoform-specific sodium channel targeting." In: *Journal of Neuroscience* 23.6 (2003), pp. 2306–2313.

[50] Wenqin Hu, Cuiping Tian, Tun Li, Mingpo Yang, Han Hou, and Yousheng Shu. "Distinct contributions of Na v 1.6 and Na v 1.2 in action potential initiation and backpropagation." In: *Nature neuroscience* 12.8 (2009), pp. 996–1002.

[51] Indira M Raman and Bruce P Bean. "Resurgent sodium current and action potential formation in dissociated cerebellar Purkinje neurons." In: *Journal of Neuroscience* 17.12 (1997), pp. 4517–4526.

[52] Wilfried A Kues and Frank Wunder. "Heterogeneous expression patterns of mammalian potassium channel genes in developing and adult rat brain." In: *European Journal of Neuroscience* 4.12 (1992), pp. 1296–1308.

[53] Rüdiger W Veh, Ralf Lichtinghagen, Sabine Sewing, Frank Wunder, Isabella M Grumbach, and Olaf Pongs. "Immunohistochemical localization of five members of the Kv1 channel subunits: contrasting subcellular locations and neuron-specific co-localizations in rat brain." In: *European Journal of Neuroscience* 7.11 (1995), pp. 2189–2205.

[54] Andrea Lorincz and Zoltan Nusser. "Molecular identity of dendritic voltage-gated sodium channels." In: *Science* 328.5980 (2010), pp. 906–909.

[55] E Benoit and JM Dubois. "Properties of maintained sodium current induced by a toxin from Androctonus scorpion in frog node of Ranvier." In: *The Journal of physiology* 383.1 (1987), pp. 93–114.

[56] JM Dubois and C Bergman. "Late sodium current in the node of Ranvier." In: *Pflügers Archiv* 357.1 (1975), pp. 145–148.

[57] Richard Fitzhugh. "Computation of impulse initiation and saltatory conduction in a myelinated nerve fiber." In: *Biophysical journal* 2.1 (1962), pp. 11–21.

[58] L Goldman and James S Albus. "Computation of impulse conduction in myelinated fibers; theoretical basis of the velocity-diameter relation." In: *Biophysical journal* 8.5 (1968), pp. 596–607.

[59] Donald R McNeal. "Analysis of a model for excitation of myelinated nerve." In: *IEEE Transactions on Biomedical Engineering* 4 (1976), pp. 329–337.

[60] JD Sweeney, JT Mortimer, and D Durand. "Modeling of mammalian myelinated nerve for functional neuromuscular stimulation." In: *IEEE 9th Annual Conference of the Engineering in Medicine and Biology Society*. Vol. 3. 1987, pp. 1577–1578.

[61] John W Moore, Ronald W Joyner, Micheal H Brill, Stephen D Waxman, and Manuel Najar-Joa. "Simulations of conduction in uniform myelinated fibers. Relative sensitivity to changes in nodal and internodal parameters." In: *Biophysical journal* 21.2 (1978), pp. 147–160.

[62] JOSEPH Patlak. "Molecular kinetics of voltage-dependent Na+ channels." In: *Physiological reviews* 71.4 (1991), pp. 1047–1080.

[63] Joseph Xu Zhou, Xiaojie Qiu, Aymeric Fouquier d'Hérouël, and Sui Huang. "Discrete gene network models for understanding multicellularity and cell reprogramming: from network structure to attractor landscape." In: *Computational Systems Biology* (2014), pp. 241–276.

[64] Edward Vigmond and Gernot Plank. "Cardiac Modeling." In: (2019).

[65] Cameron C McIntyre and Warren M Grill. "Sensitivity analysis of a model of mammalian neural membrane." In: *Biological cybernetics* 79.1 (1998), pp. 29–37.

[66] SY Chiu, JM Ritchie, RB Rogart, and D Stagg. "A quantitative description of membrane currents in rabbit myelinated nerve." In: *The Journal of physiology* 292.1 (1979), pp. 149–166.

[67] Martin Pospischil, Maria Toledo-Rodriguez, Cyril Monier, Zuzanna Piwkowska, Thierry Bal, Yves Frégnac, Henry Markram, and Alain Destexhe. "Minimal Hodgkin–Huxley type models for different classes of cortical and thalamic neurons." In: *Biological cybernetics* 99.4 (2008), pp. 427–441.

[68] Pietro Balbi, Paolo Massobrio, and Jeanette Hellgren Kotaleski. "A single Markov-type kinetic model accounting for the macroscopic currents of all human voltage-gated sodium channel isoforms." In: *PLoS computational biology* 13.9 (2017), e1005737.

[69] Bin Feng, Yi Zhu, Jun-Ho La, Zachary P Wills, and Gerald F Gebhart. "Experimental and computational evidence for an essential role of NaV1. 6 in spike initiation at stretch-sensitive colorectal afferent endings." In: *Journal of neurophysiology* 113.7 (2015), pp. 2618–2634.

[70] Colin Peters, Richard E Rosch, Elaine Hughes, and Peter C Ruben. "Temperature-dependent changes in neuronal dynamics in a patient with an SCN1A mutation and hyperthermia induced seizures." In: *Scientific reports* 6.1 (2016), pp. 1–12.

[71] Mingyu Ye, Jun Yang, Cuiping Tian, Qiyu Zhu, Luping Yin, Shan Jiang, Mingpo Yang, and Yousheng Shu. "Differential roles of Na V 1.2 and Na V 1.6 in regulating neuronal excitability at febrile temperature and distinct contributions to febrile seizures." In: *Scientific reports* 8.1 (2018), pp. 1–15.

[72] Rajnish Ranjan, Emmanuelle Logette, Michela Marani, Mirjia Herzog, Valérie Tâche, Enrico Scantamburlo, Valérie Buchillier, and Henry Markram. "A kinetic map of the homomeric voltage-gated potassium channel (Kv) family." In: *Frontiers in cellular neuroscience* 13 (2019), p. 358.

[73] Rajnish Ranjan, Georges Khazen, Luca Gambazzi, Srikanth Ramaswamy, Sean L Hill, Felix Schürmann, and Henry Markram. "Channelpedia: an integrative and interactive database for ion channels." In: *Frontiers in neuroinformatics* 5 (2011), p. 36.

[74] DK Sharma and Akhil Ranjan Garg. "Dynamics of HH Model for Excitable Neuron with Added Voltage Gated Calcium Channel." In: *International Journal of Computer Applications* 975 (2014), p. 8887.

[75] Gregory M Faber, Jonathan Silva, Leonid Livshitz, and Yoram Rudy. "Kinetic properties of the cardiac L-type Ca2+ channel and its role in myocyte electrophysiology: a theoretical investigation." In: *Biophysical journal* 92.5 (2007), pp. 1522–1543.

[76] Alexey E Alekseev, Nick I Markevich, Antonina F Korystova, Andre Terzic, and Yuri M Kokoz. "Comparative analysis of the kinetic characteristics of L-type calcium channels in cardiac cells of hibernators." In: *Biophysical journal* 70.2 (1996), pp. 786–797.

[77] B Frankenhaeuser and AF Huxley. "The action potential in the myelinated nerve fibre of Xenopus laevis as computed on the basis of voltage clamp data." In: *The Journal of Physiology* 171.2 (1964), pp. 302–315.

[78] J Patrick Reilly, Vanda T Freeman, and Willard D Larkin. "Sensory effects of transient electrical stimulation-evaluation with a neuroelectric model." In: *IEEE transactions on biomedical engineering* 12 (1985), pp. 1001–1011.

[79] Peter H Gorman and J Thomas Mortimer. "The effect of stimulus parameters on the recruitment characteristics of direct nerve stimulation." In: *IEEE Transactions on Biomedical Engineering* 7 (1983), pp. 407–414.

[80] JH Meier, WLC Rotten, AE Zoutman, HBK Boom, and P Bergveld. "Simulation of multipolar fiber selective neural stimulation using intrafascicular electrodes." In: *IEEE Transactions on Biomedical Engineering* 39.2 (1992), pp. 122–134.

[81] JHM Frijns and JH Ten Kate. "A model of myelinated nerve fibres for electrical prosthesis design." In: *Medical and Biological Engineering and Computing* 32.4 (1994), pp. 391–398.

[82] Gordon M Schoepfle and Joseph Erlanger. "The action of temperature on the excitability, spike height and configuration, and the refractory period observed in the responses of single medullated nerve fibers." In: *American Journal of Physiology-Legacy Content* 134.4 (1941), pp. 694–704.

[83] Cameron C McIntyre et al. "Modeling the excitability of mammalian nerve fibers: influence of afterpotentials on the recovery cycle." In: *Journal of neurophysiology* 87.2 (2002), pp. 995–1006.

[84] Ellen F Barrett and John N Barrett. "Intracellular recording from vertebrate myelinated axons: mechanism of the depolarizing afterpotential." In: *The Journal of physiology* 323.1 (1982), pp. 117–144.

[85] AR Blight and S Someya. "Depolarizing afterpotentials in myelinated axons of mammalian spinal cord." In: *Neuroscience* 15.1 (1985), pp. 1–12.

[86] AR Blight. "Computer simulation of action potentials and afterpotentials in mammalian myelinated axons: the case for a lower resistance myelin sheath." In: *Neuroscience* 15.1 (1985), pp. 13–31.

[87] F Awiszus. "Effects of paranodal potassium permeability on repetitive activity of mammalian myelinated nerve fiber models." In: *Biological cybernetics* 64.1 (1990), pp. 69–76.

[88] John Alan Halter and John W Clark Jr. "A distributed-parameter model of the myelinated nerve fiber." In: *Journal of theoretical biology* 148.3 (1991), pp. 345–382.

[89] H Bostock, M Baker, and G Reid. "Changes in excitability of human motor axons underlying post-ischaemic fasciculations: evidence for two stable states." In: *The Journal of Physiology* 441.1 (1991), pp. 537–557.

[90] DI Stephanova and H Bostock. "A distributed-parameter model of the myelinated human motor nerve fibre: temporal and spatial distributions of action potentials and ionic currents." In: *Biological cybernetics* 73.3 (1995), pp. 275–280.

[91] AG Richardson, CC McIntyre, and WM Grill. "Modelling the effects of electric fields on nerve fibres: influence of the myelin sheath." In: *Medical and Biological Engineering and Computing* 38.4 (2000), pp. 438–446.

[92] Jürgen R Schwarz, Gordon Reid, and Hugh Bostock. "Action potentials and membrane currents in the human node of Ranvier." In: *Pflügers Archiv* 430.2 (1995), pp. 283–292.

[93] BV Safronov, K Kampe, and W Vogel. "Single voltage-dependent potassium channels in rat peripheral nerve membrane." In: *The Journal of physiology* 460.1 (1993), pp. 675–691.

[94] Kaihua Zhu, Liming Li, Xuyong Wei, and Xiaohong Sui. "A 3D computational model of transcutaneous electrical nerve stimulation for estimating Aβ tactile nerve fiber excitability." In: *Frontiers in neuroscience* 11 (2017), p. 250.

[95] Christopher W Elder and Paul B Yoo. "A finite element modeling study of peripheral nerve recruitment by percutaneous tibial nerve stimulation in the human lower leg." In: *Medical engineering & physics* 53 (2018), pp. 32–38.

[96] Andreas Kuhn, Thierry Keller, Marc Lawrence, and Manfred Morari. "A model for transcutaneous current stimulation: simulations and experiments." In: *Medical & biological engineering & computing* 47.3 (2009), pp. 279–289.

[97] Matthew A Schiefer, Ronald J Triolo, and Dustin J Tyler. "A model of selective activation of the femoral nerve with a flat interface nerve electrode for a lower extremity neuroprosthesis." In: *IEEE transactions on neural systems and rehabilitation engineering* 16.2 (2008), pp. 195–204.

[98] Peter Schier, Michael Handler, Lejo Johnson Chacko, Anneliese Schrott-Fischer, Karl Fritscher, Rami Saba, Christian Baumgartner, and Daniel Baumgarten. "Model-based vestibular afferent stimulation: evaluating selective electrode locations and stimulation waveform shapes." In: *Frontiers in neuroscience* 12 (2018), p. 588.

[99] Adam Q Choi, James K Cavanaugh, and Dominique M Durand. "Selectivity of multiple-contact nerve cuff electrodes: a simulation analysis." In: *IEEE Transactions on Biomedical Engineering* 48.2 (2001), pp. 165–172.

[100] Chad A Bossetti et al. "Analysis of the quasi-static approximation for calculating potentials generated by neural stimulation." In: *Journal of neural engineering* 5.1 (2007), p. 44.

[101] F Kolbl, M Capllonch Juan, and Francisco Sepulveda. "Impact of the angle of implantation of transverse intrafascicular multichannel electrodes on axon activation." In: *2016 IEEE Biomedical Circuits and Systems Conference (BioCAS)*. IEEE. 2016, pp. 484–487.

[102] Javier Perez-Orive and DM Durund. "Modeling study of peripheral nerve recording selectivity." In: *IEEE Transactions on Rehabilitation Engineering* 8.3 (2000), pp. 320–329.

[103] Carl H Lubba, Yann Le Guen, Sarah Jarvis, Nick S Jones, Simon C Cork, Amir Eftekhar, and Simon R Schultz. "PyPNS: Multiscale simulation of a peripheral nerve in python." In: *Neuroinformatics* 17.1 (2019), pp. 63–81.

[104] Anil Kumar RamRakhyani, Zachary B Kagan, David J Warren, Richard A Normann, and Gianluca Lazzi. "A μm-Scale Computational Model of Magnetic Neural Stimulation in Multifascicular Peripheral Nerves." In: *IEEE Transactions On Biomedical Engineering* 62.12 (2015), pp. 2837–2849.

[105] Simone Romeni et al. "Tutorial: a computational framework for the design and optimization of peripheral neural interfaces." In: *Nat. Prot.* 15.10 (2020), pp. 3129–3153.

[106] Michael L Hines and Nicholas T Carnevale. "The NEURON simulation environment." In: *Neural computation* 9.6 (1997), pp. 1179–1209.

[107] Wigand Poppendieck et al. "A new generation of double-sided intramuscular electrodes for multi-channel recording and stimulation." In: *EMBC Conference*. 2015.

[108] Michael E Jabaley, William H Wallace, and Frederick R Heckler. "Internal topography of major nerves of the forearm and hand: a current view." In: *The Journal of hand surgery* 5.1 (1980), pp. 1–18.

[109] Natalie A Brill and Dustin J Tyler. "Quantification of human upper extremity nerves and fascicular anatomy." In: *Muscle & nerve* 56.3 (2017), pp. 463–471.

[110] Ake B Vallbo, Roland S Johansson, et al. "Properties of cutaneous mechanoreceptors in the human hand related to touch sensation." In: *Hum Neurobiol* 3.1 (1984), pp. 3–14.

[111] Gal Ohad. *https://www.mathworks.com/matlabcentral/fileexchange/3215-fit_ellipse*.

[112] Ignacio Delgado-Martínez, Jordi Badia, Arán Pascual-Font, Alfonso Rodríguez-Baeza, and Xavier Navarro. "Fascicular topography of the human median nerve for neuroprosthetic surgery." In: *Frontiers in neuroscience* 10 (2016), p. 286.

[113] Alexander R Kent and Warren M Grill. "Model-based analysis and design of nerve cuff electrodes for restoring bladder function by selective stimulation of the pudendal nerve." In: *Journal of neural engineering* 10.3 (2013), p. 036010.

[114] Felipe Fregni and Alvaro Pascual-Leone. "Technology insight: noninvasive brain stimulation in neurology—perspectives on the therapeutic potential of rTMS and tDCS." In: *Nature clinical practice Neurology* 3.7 (2007), pp. 383–393.

[115] Mark S George and Gary Aston-Jones. "Noninvasive techniques for probing neurocircuitry and treating illness: vagus nerve stimulation (VNS), transcranial magnetic stimulation (TMS) and transcranial direct current stimulation (tDCS)." In: *Neuropsychopharmacology* 35.1 (2010), pp. 301–316.

[116] Kate E Hoy and Paul B Fitzgerald. "Brain stimulation in psychiatry and its effects on cognition." In: *Nature Reviews Neurology* 6.5 (2010), pp. 267–275.

[117] Colleen K Loo and Philip B Mitchell. "A review of the efficacy of transcranial magnetic stimulation (TMS) treatment for depression, and current and future strategies to optimize efficacy." In: *Journal of affective disorders* 88.3 (2005), pp. 255–267.

[118] Yusuf Tufail, Alexei Matyushov, Nathan Baldwin, Monica L Tauchmann, Joseph Georges, Anna Yoshihiro, Stephen I Helms Tillery, and William J Tyler. "Transcranial pulsed ultrasound stimulates intact brain circuits." In: *Neuron* 66.5 (2010), pp. 681–694.

[119] Randy L King, Julian R Brown, William T Newsome, and Kim Butts Pauly. "Effective parameters for ultrasound-induced in vivo neurostimulation." In: *Ultrasound in medicine & biology* 39.2 (2013), pp. 312–331.

[120] Seung-Schik Yoo, Alexander Bystritsky, Jong-Hwan Lee, Yongzhi Zhang, Krisztina Fischer, Byoung-Kyong Min, Nathan J McDannold, Alvaro Pascual-Leone, and Ferenc A Jolesz. "Focused ultrasound modulates region-specific brain activity." In: *Neuroimage* 56.3 (2011), pp. 1267–1275.

[121] Thomas Deffieux, Youliana Younan, Nicolas Wattiez, Mickael Tanter, Pierre Pouget, and Jean-François Aubry. "Low-intensity focused ultrasound modulates monkey visuomotor behavior." In: *Current Biology* 23.23 (2013), pp. 2430–2433.

[122] Wynn Legon, Leo Ai, Priya Bansal, and Jerel K Mueller. "Neuromodulation with single-element transcranial focused ultrasound in human thalamus." In: *Human brain mapping* 39.5 (2018), pp. 1995–2006.

[123] Wonhye Lee, Hyun-Chul Kim, Yujin Jung, Yong An Chung, In-Uk Song, Jong-Hwan Lee, and Seung-Schik Yoo. "Transcranial focused ultrasound stimulation of human primary visual cortex." In: *Scientific reports* 6.1 (2016), pp. 1–12.

[124] Leo Ai, Jerel K Mueller, Andrea Grant, Yigitcan Eryaman, and Wynn Legon. "Transcranial focused ultrasound for BOLD fMRI signal modulation in humans." In: *2016 38th Annual International Conference of the IEEE Engineering in Medicine and Biology Society (EMBC)*. IEEE. 2016, pp. 1758–1761.

[125] Stuart Hameroff, Michael Trakas, Chris Duffield, Emil Annabi, M Bagambhrini Gerace, Patrick Boyle, Anthony Lucas, Quinlan Amos, Annemarie Buadu, and John J Badal. "Transcranial ultrasound (TUS) effects on mental states: a pilot study." In: *Brain stimulation* 6.3 (2013), pp. 409–415.

[126] Wonhye Lee, Hyungmin Kim, Yujin Jung, In-Uk Song, Yong An Chung, and Seung-Schik Yoo. "Image-guided transcranial focused ultrasound stimulates human primary somatosensory cortex." In: *Scientific reports* 5.1 (2015), pp. 1–10.

[127] Jerel Mueller, Wynn Legon, Alexander Opitz, Tomokazu F Sato, and William J Tyler. "Transcranial focused ultrasound modulates intrinsic and evoked EEG dynamics." In: *Brain stimulation* 7.6 (2014), pp. 900–908.

[128] Wynn Legon, Tomokazu F Sato, Alexander Opitz, Jerel Mueller, Aaron Barbour, Amanda Williams, and William J Tyler. "Transcranial focused ultrasound modulates the activity of primary somatosensory cortex in humans." In: *Nature neuroscience* 17.2 (2014), pp. 322–329.

[129] Benjamin C Gibson, Joseph L Sanguinetti, Bashar W Badran, Alfred B Yu, Evan P Klein, Christopher C Abbott, Jeffrey T Hansberger, and Vincent P Clark. "Increased excitability induced in the primary motor cortex by transcranial ultrasound stimulation." In: *Frontiers in neurology* 9 (2018), p. 1007.

[130] Jerel K Mueller, Leo Ai, Priya Bansal, and Wynn Legon. "Computational exploration of wave propagation and heating from transcranial focused ultrasound for neuromodulation." In: *Journal of neural engineering* 13.5 (2016), p. 056002.

[131] Jerel K Mueller, Leo Ai, Priya Bansal, and Wynn Legon. "Numerical evaluation of the skull for human neuromodulation with transcranial focused ultrasound." In: *Journal of neural engineering* 14.6 (2017), p. 066012.

[132] Luis Vargas, He Helen Huang, Yong Zhu, and Xiaogang Hu. "Merged haptic sensation in the hand during concurrent Non-Invasive proximal nerve stimulation." In: *2018 40th Annual International Conference of the IEEE Engineering in Medicine and Biology Society (EMBC)*. IEEE. 2018, pp. 2186–2189.

[133] Christian Antfolk, Marco D'alonzo, Birgitta Rosén, Göran Lundborg, Fredrik Sebelius, and Christian Cipriani. "Sensory feedback in upper limb prosthetics." In: *Expert review of medical devices* 10.1 (2013), pp. 45–54.

[134] Bradley E Treeby and Ben T Cox. "Modeling power law absorption and dispersion in viscoelastic solids using a split-field and the fractional Laplacian." In: *The Journal of the Acoustical Society of America* 136.4 (2014), pp. 1499–1510.

[135] Cecile Baron, Jean-François Aubry, Mickael Tanter, Stephen Meairs, and Mathias Fink. "Simulation of intracranial acoustic fields in clinical trials of sonothrombolysis." In: *Ultrasound in medicine & biology* 35.7 (2009), pp. 1148–1158.

[136] Michael Plaksin, Shy Shoham, and Eitan Kimmel. "Intramembrane cavitation as a predictive bio-piezoelectric mechanism for ultrasonic brain stimulation." In: *Physical review X* 4.1 (2014), p. 011004.